Review

Thermal Management Technologies Used for High Heat Flux Automobiles and Aircraft: A Review

Yi-Gao Lv [1], Gao-Peng Zhang [2], Qiu-Wang Wang [1] and Wen-Xiao Chu [1,*]

[1] Key Laboratory of Thermo-Fluid Science and Engineering, Ministry of Education, Xi'an Jiaotong University, Xi'an 710049, China
[2] Xi'an Institute of Optics and Precision Mechanics, Chinese Academy of Sciences (CAS), Xi'an 710119, China
* Correspondence: wxchu84@xjtu.edu.cn

Abstract: In recent years, global automotive industries are going through a significant revolution from traditional internal combustion engine vehicles (ICEVs) to electric vehicles (EVs) for CO_2 emission reduction. Very similarly, the aviation industry is developing towards more electric aircraft (MEA) in response to the reduction in global CO_2 emission. To promote this technology revolution and performance advancement, plenty of electronic devices with high heat flux are implemented on board automobiles and aircraft. To cope with the thermal challenges of electronics, in addition to developing wide bandgap (WBG) semiconductors with satisfactory electric and thermal performance, providing proper thermal management solutions may be a much more cost-effective way at present. This paper provides an overview of the thermal management technologies for electronics used in automobiles and aircraft. Meanwhile, the active methods include forced air cooling, indirect contact cold plate cooling, direct contact baseplate cooling, jet impingement, spray cooling, and so on. The passive methods include the use of various heat pipes and PCMs. The features, thermal performance, and development tendency of these active and passive thermal management technologies are reviewed in detail. Moreover, the environmental influences introduced by vibrations, shock, acceleration, and so on, on the thermal performance and reliability of the TMS are specially emphasized and discussed in detail, which are usually neglected in normal operating conditions. Eventually, the possible future directions are discussed, aiming to serve as a reference guide for engineers and promote the advancement of the next-generation electronics TMS in automobile and aircraft applications.

Keywords: thermal management; automobile; aircraft; active cooling; passive cooling; environmental influences

Citation: Lv, Y.-G.; Zhang, G.-P.; Wang, Q.-W.; Chu, W.-X. Thermal Management Technologies Used for High Heat Flux Automobiles and Aircraft: A Review. *Energies* **2022**, *15*, 8316. https://doi.org/10.3390/en15218316

Academic Editor: Massimiliano Renzi

Received: 19 September 2022
Accepted: 4 November 2022
Published: 7 November 2022

Publisher's Note: MDPI stays neutral with regard to jurisdictional claims in published maps and institutional affiliations.

Copyright: © 2022 by the authors. Licensee MDPI, Basel, Switzerland. This article is an open access article distributed under the terms and conditions of the Creative Commons Attribution (CC BY) license (https://creativecommons.org/licenses/by/4.0/).

1. Introduction

Nowadays, elevated concerns about the global environment caused by greenhouse gas emissions have stimulated a growing demand for sustainable energy development. As a result, global automotive industries are exhibiting a significant revolution from traditional internal combustion engine vehicles (ICEVs) to electric vehicles (EVs), including hybrid electric vehicles (HEVs) and all electric vehicles (AEVs). Figure 1 shows a schematic diagram of an HEV [1]. As regards ICEVs and HEVs, great efforts in new technical innovation on improving engine efficiency and fuel economy were made by introducing electrification components for the replacement of traditional mechanical components. However, the current near-engine trend and the necessity to place the engine control unit (ECU) on the engine and transmission control unit (TCU) close to the transmission will raise the ambient temperature of electronics to the level above 125 °C. According to a summary of automotive electronics requirement, as shown in Table 1, the ambient temperature for most parts of the cavity under the hood may exceed 150 °C [2].

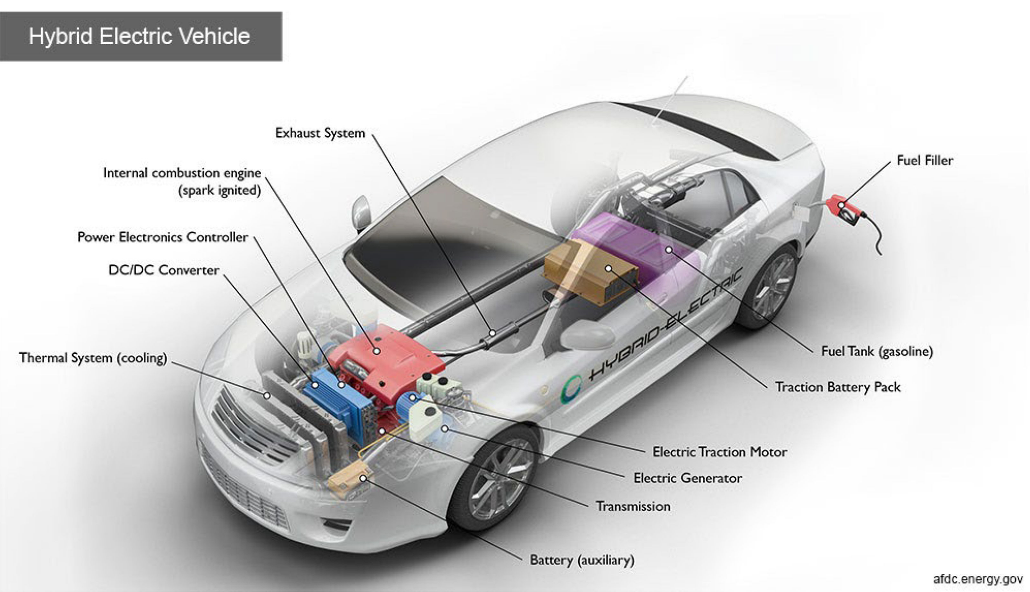

Figure 1. Schematic diagram of an HEV [1].

Table 1. Maximum temperature ranges of automotive with engine [2].

Locations	Temperature Range
On engine	150–200 °C
In transmission	150–200 °C
On wheel ABS sensors	150–250 °C
Cylinder pressure	200–300 °C
Exhaust sensing	Up to 850 °C, ambient 300 °C

On the other hand, with respect to EVs, the large amount of heat dissipated from either the engine or the high-power electric traction motor and other devices will also generate a high-temperature environment. Over the last decade, the EV market has driven the marketplace of power electronic modules with high heat flux. Typical power electronics in these modules, such as diodes, metal–oxide–semiconductor field-effect transistors (MOSFETs), and insulated gate bipolar transistors (IGBTs), operate under a high-temperature environment [3]. The junction temperatures of these electronics usually operate up to 15 °C higher than the ambient temperature. Moreover, this value can even reach 25 °C for power devices. As a result, electronics under the hood of vehicles, especially those placed close to the engine, suffer from work temperatures over 175 °C, thus severely threatening the reliability and service life of these electronics [4].

To tackle this issue, several measures have been proposed, such as increasing the silicon die area of the device, applying a device made of wide-bandgap (WBG) semiconductor materials, such as SiC and GaN, which are capable of operating at 175 to 200 °C [5–9]. For example, Huque et al. [2] newly designed a gate-driven integrated circuit for SiC transistor switches. They successfully tested a prototype chip at ambient temperature up to 200 °C without taking any cooling measure. Although SiC modules were built with high-temperature packages, the cost of most advanced semiconductor devices remains prohibitive for commercial use, and even military products are still in the early prototype phase [10]. In this regard, it is crucial to design a cost-effective thermal management system (TMS) with high safety and reliability for power electronics under the hood. Meanwhile, the temperature requirements and the total cost of electronic modules can be apparently reduced by providing effective thermal management for the modules [11]. In a word, the application of effective thermal management strategies can improve intrinsic reliability, reduce thermal strains, and make the use of commercial off-the-shelf modules considerably more attractive. On the other hand, the cost is also an important driving factor in automotive industries. Moreover, the future development trends of automotive electric

devices favor higher speeds and smaller sizes accompanied by better performance, which will accordingly raise the heat generation rates of ECU and TCU, thus leading to more strict requirements of thermal management techniques [12]. In addition to the high ambient temperature, many other environmental factors, such as vibration and abrupt acceleration, may also affect the reliability and performance of electric devices and related TMS [13]. When powertrain electronics are mounted directly onto ICEs and transmissions, some concerns about powertrain electronics might simultaneously occur due to vibrations, eventually leading to damage of the structural integrity and performance deterioration of the electronics. Moreover, different from commercial vehicles, military combat vehicles could even have additional shock sources from ballistic launch, gun firing, abrupt maneuvering, and so on [14]. This can pose more severe challenges to the design of the TMS.

Very similar to the automotive industry, the aviation industry is also facing challenges in providing reliable thermal management for electronics under a harsh environment. In order to minimize the wiring length of actuators and sensors, the ECU of an aero engine is typically mounted on the engine case [15]. As a result, the ECU will be exposed to a high-temperature and high-vibration environment. Moreover, the dense circuit packaging because of the aerospace sensitivity to equipment size and weight, as well as the required high processor throughput, will lead to much higher heat flux [16]. On the other hand, more electric aircraft (MEA) are also being developed in response to the reduction in global CO_2 emission [17,18]. Note that the power requirement can be reduced, and lower fuel burn and CO_2 emissions can be achieved by developing MEA [19]. To achieve this goal, stringent requirements are placed on the reliability of power electronic components integrated with novel high-power electric machines. Note that while a large amount of literature focuses on automobiles, investigations on MEA and electric propulsion have been conducted only for several years in the aviation industry. However, compared with automobiles, what makes the thermal management of electronics on board aircraft much more complicated is that heat sinks of the aircraft TMS are very limited [20]. Figure 2 shows the distribution of different types of heat sink in a modern aircraft, and the locations and basic configuration of these heat sinks are also illustrated. These five heat sinks are ram air, engine fan air, skin heat exchanger, expendable heat sink, and fuel [20]. Among these heat sinks, the fuel, which is typically stored in the fuel tank system, is the most significant one [21]. In normal operation mode, the waste heat collected by the fuel is then rejected via a burning process in the engine or recovered to the tank [21].

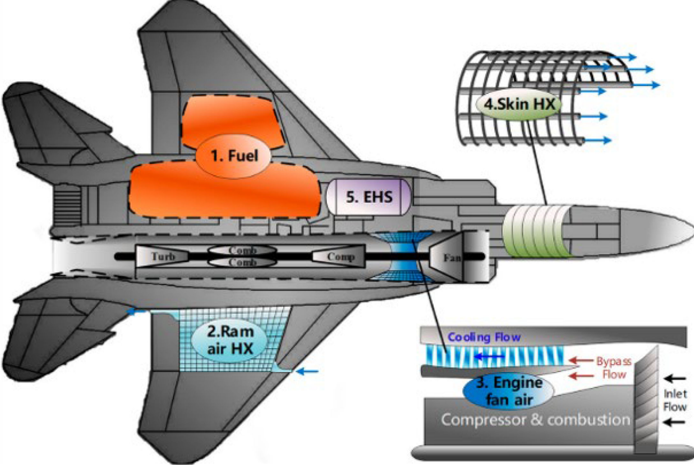

Figure 2. Typical heat sinks in a modern aircraft [20].

Based on the above discussion, it can be found that the thermal management concerns for automobiles and aircraft present high similarity in terms of the implemented electronics and the typical design constraints posed under a harsh operating environment, as summarized in Table 2. Thus, the thermal management technologies for electronics used in these

two fields are discussed together. Note that the TMS of an aircraft is much more sensitive to the system mass and volume. Actually, thermal management is considered to be one of the most difficult challenges for advanced aircraft design.

Table 2. Design features of the TMS for electronics used in automobiles and aircraft.

Industrial Field	Development Tendency	Environmental Constraints and Design Considerations
Automotive	HEV; AEV	High temperature, limited space, limited applicable coolant, vibration, acceleration, shock
Aviation	MEA	Limited heat sink, high temperature, vibration, loss/hypergravity, very sensitive to system mass and volume.

In order to provide reliable and effective thermal management for electronics used in automobiles and aircraft, scientists proposed lots of strategies over the last decades, including forced air cooling, forced liquid cooling, jet impingement, spray cooling, and so on. Forced liquid cooling is the most widely adopted one, which can be divided into two categories, namely, indirect contact cold plate cooling and direct contact baseplate cooling. Besides, some other techniques, such as heat pipes, thermoelectric coolers (TECs), and phase change materials (PCMs), were also adopted in the TMS. Table 3 summarizes a review of literature related to the thermal management of electronics used in automobiles and aircraft. It can be observed that the environmental factors (vibration, shock, acceleration, etc.) that may significantly affect the thermal performance and reliability of the TMS are usually neglected [22–27]. To bridge this gap, the thermal management technologies for electronics on board automobiles and aircraft are systematically reviewed as the outline shown in Figure 3. The structural characteristics, thermal performance, and development tendency of the active and passive thermal management technologies are introduced in detail. Moreover, the environmental influences posed by the harsh operating environment on the thermal performance and reliability of the TMS are discussed and emphasized.

Table 3. Summary of the previous reviews concerning the TMS for electronics on board automobiles and aircraft.

Reference	Topics	Major Contents
Zuo et al. in 2008 [28]	HEV/AEV	• Several advanced heat pipes used for heat spreading, heat transport, and temperature control.
Nakayama et al. in 2009 [3]	HEV/AEV	• Tools for thermal design analysis.
Jankowski et al. in 2014 [10]	ICEV/HEV/AEV	• PCMs used for vehicle component thermal buffering with respect to different temperature ranges.
Broughton et al. in 2017 [29]	HEV/AEV	• Evolution of thermal packaging in HEVs and AEVs. • Thermal packaging options for Si and SiC power modules.
Antti et al. in 2018 [30]	HEV/AEV	• Comparison of different thermal management systems based on various vehicle configurations. • Discussion on various vehicle thermal management modeling techniques. • Thermal management of various powertrain components including the internal combustion engine, battery, electric machines, and power electronics.
López et al. in 2019 [31]	HEV/AEV	• Various EV propulsion architectures and enabling technologies for next-generation drives. • Next-generation electric machines for EV and HEV propulsion systems. • WBG semiconductor-based power control units for automotive drive systems. • Thermal management technologies for power converter.

Table 3. *Cont.*

Reference	Topics	Major Contents
Marshall et al. in 2019 [32]	ICEV/HEV/AEV	• Thermal management of vehicle cabins, external components, and onboard electronics of vehicles.
Oh et al. in 2019 [33]	ICEV/HEV/AEV	• A survey of various thermal metrology techniques used for studying GaN-based electronics and photonics. • Practical thermal management solutions for GaN-based power electronics. • Packaging techniques and cooling systems for GaN-based LEDs applied for automotive lighting.
Lu in 2020 [34]	HEV/AEV	• Analysis of power modules used in commercial traction inverters.
Yuan et al. in 2020 [35]	HEV	• Latest techniques for vehicle powertrain modelling. • Vehicle body thermal model including the cabin thermal model and under-hood heat retention model. • Holistic modelling and cosimulation techniques used for thermal energy management in a hybrid vehicle.
Abramushkina et al. in 2021 [36]	HEV/AEV	• Introduction of new WBG semiconductors with a focus on their thermal properties. • Assess various inverter cooling methods including air cooling, liquid cooling, and heat pipes.
Jones-Jackson et al. in 2021 [37]	HEV/AEV	• Discuss the jet cooling characteristics for automotive applications including the heat transfer, pressure drop, and reliability. • Outline the advanced jet impingement technology investigated in electric vehicle power modules.
Previati et al. in 2022 [38]	HEV/AEV	• Thermal management requirements and the basic architectures of different electrified vehicle subsystems. • Analyze the main components of the vehicle and describe the related challenges and modeling issues.
Freeman et al. in 2014 [39]	MEA/HEA/AEA	• Architecture-level analysis of the coupled relationship between different subsystems of advanced aircraft.
Pal et al. in 2017 [21]	MEA	• Discuss various cooling architectures of power electronics in a system level. Advantages and disadvantages of these cooling schemes are described.
McCluskey et al. in 2018 [17]	MEA/HEA	• Discuss different cooling technologies' target for high heat fluxes devices.
Hendricks et al. in 2021 [40]	HEA	• Introduce the overall aircraft thermal management architectures. • Discuss the advanced thermal energy capture and transport technologies and the advanced aircraft exhaust heat recovery technologies.
Wang et al. in 2021 [41]	Aerospace vehicles	• Elaborate the available onboard heat sinks and aerospace thermal management systems. • Introduce the development of aerospace active TMSs in China.
Wileman et al. in 2021 [19]	MEA	• Examine the current architecture of the MEA and the various power electronic failure modes. • Discuss the reliability of these electrified systems.
Heerden et al. in 2022 [18]	MEA/HEA/AEA	• Present challenges and opportunities of the aircraft TMS in detail. • Discuss several topics of particular priority in thermal management research for aircraft.

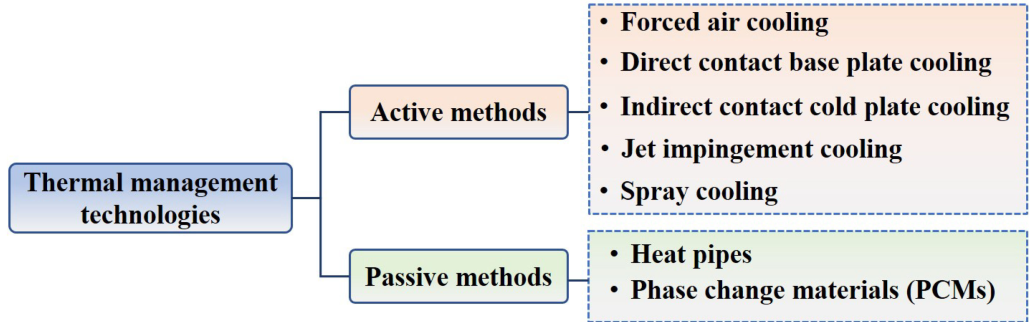

Figure 3. Thermal management technologies applicable for electronics on board automobiles and aircraft.

2. Active Methods

2.1. Forced Air Cooling

In general, the forced air cooling is seldom implemented for traditional silicon-based power electronics in HEV/AEVs because of its apparently lower heat transfer efficiency in comparison with the commonly used liquid cooling scheme. In fact, the air remains the ultimate destination for all heat rejected from the vehicle. The direct use of air for cooling exhibits some advantages in improving the compactness and reducing the complexity and cost via the elimination of an additional cooling loop and many bulky components. Thus, the forced air cooling remains competitive for the thermal management of advanced traction drive inverters. In recent years, the emergence of WBG semiconductors, such as SiC, which are capable of operating at a higher temperature, makes the forced air cooling technology promising in the TMS without sacrificing drive performance [42]. As a result, commercial HEVs are preferred to adopt air-cooled inverters, and considerable engineers focus on the development of the forced air cooling for vehicles using WBG semiconductors. Table 4 summarizes studies focusing on the forced air cooling for automotive power electronics.

Table 4. Summary of studies focusing on the forced air cooling for automotive power electronics.

Reference	Target Devices	Allowable Junction Temperature	Ambient Temperature	Maximum Device Temperature
Chinthavali et al. [43]	SiC-based automotive traction drive inverter	N/A	120 °C	164 °C
Sato et al. [44]	SiC-based inverter for motor drive applications	200 °C	25 °C	N/A
Wrzecionko et al. [45]	SiC-based automotive inverter	175 °C for first prototype (250 °C for design process)	120 °C	N/A
Liu et al. [46]	SiC-based inverter	N/A	25 °C	94.4 °C
Zeng et al. [47]	SiC-based inverter	>200 °C	25 °C	Approximately 140 °C
Li et al. [48]	SiC-based DC/AC converter	N/A	40 °C	150 °C

Despite the adoption of WBG semiconductors, it remains challenging to design an air-cooled automotive inverter that keeps the overall volume comparable to a liquid cooled one. To determine the feasibility of using forced air to cool an axial flow cylindrical-shaped and rectangular-shaped SiC traction drive inverter, Chinthavali et al. [43,49] performed a parametric study with various air flow rates, ambient air temperatures, voltages, and device switching frequencies via transient and steady-state simulations. When the inverter was subject to one or multiple current cycles at an ambient temperature of 120 °C, the maximum junction temperature did not exceed 164 and 146 °C at an inlet flow rate of 270 cfm for the cylindrical-shaped and rectangular-shaped inverter, respectively. Sato et al. [44] designed and fabricated a SiC three-phase inverter applicable for motor drive using a forced air cooling technique. This inverter could operate steadily at a rated power of 10 kW at a junction temperature ranging from room temperature to 200 °C. Wrzecionko et al. [45] designed a forced air-cooled SiC automotive inverter with junction temperatures up to 250 °C. Especially, a TEC was integrated in the module to ensure the signal electronics and the DC-link capacitors operating within the specified temperature range. Liu et al. [46] designed a SiC inverter based on a highly integrated 3D packaging power

module. Numerical simulations were performed to optimize the diameter and distribution of the holes in a heat sink. Results showed that the heat sink with 36 holes and a 5 mm hole diameter exhibited the best thermal performance. When compared with the base design, a volume reduction of 37.5% and much more uniform temperature distribution could be obtained by using the forced air-cooled heat sink. Recently, Zeng et al. [47] proposed a stepwise design methodology to design a forced air-cooled SiC inverter. The feasibility of the proposed air-cooled SiC inverter was demonstrated via an experimental test of a prototype. A comprehensive comparison among the proposed air-cooled SiC inverter and two commercialized Si-based inverters using liquid cooling was performed. Results indicated that the proposed SiC inverter exhibits great advancement and could remarkably improve the power density of PCU and eliminate the complicated liquid cooling system. Li et al. [48] developed an air-cooled 500 kW SiC DC/AC converter based on electrical, thermal, and mechanical optimization. A record-high power density of 1.246 MW/m^3 and an efficiency over 98.5% were achieved via experimental test. Despite the growing studies focusing on WBG power electronics and the corresponding forced air cooling technique applicable for a high-temperature environment, a large number of in-depth studies remain to facilitate their mature commercial implementation. It should be noted that while the forced air cooling provides a viable option for WBG power electronics for automobiles, it is severely depressed in modern military aircraft because of the development of hypersonic vehicles.

2.2. Indirect Contact Cold Plate Cooling

Due to the inadequate cooling capacity of the forced air cooling technique and working fluid constraints in automobiles and aircraft, the forced liquid cooling has been the most commonly adopted method over the last decades [50]. In general, the forced liquid cooling can be divided into two categories, namely, indirect contact cold plate cooling and direct contact baseplate cooling, as explained in Figure 4. In terms of the indirect cold plate cooling method, the power module is not in direct contact with the coolant. By covering the cold plate, heat is absorbed by the working fluid from the devices and then rejected to the downstream heat sinks. In contrast, the baseplate and heat sink are integrated into one component for the direct contact baseplate cooling scheme. In this way, the coolant absorbs heat via the directly contact with the baseplate [51]. Hence, the extra thermal interface materials (TIMs) and heat spreaders are eliminated, and the heat transfer path is shortened accordingly. Consequently, the heat transfer efficiency can be significantly improved. In general, the indirect contact cold plate cooling technique has attracted the most attention because of its superior advantages in high stability, high controllability, and high scalability [52–54]. Table 5 summarizes studies focusing on indirect contact cold plate cooling. As far as the cold plate technique is concerned, the single-phase cold plate and the two-phase cold plate are usually categorized by the presence of a phase change of working fluid.

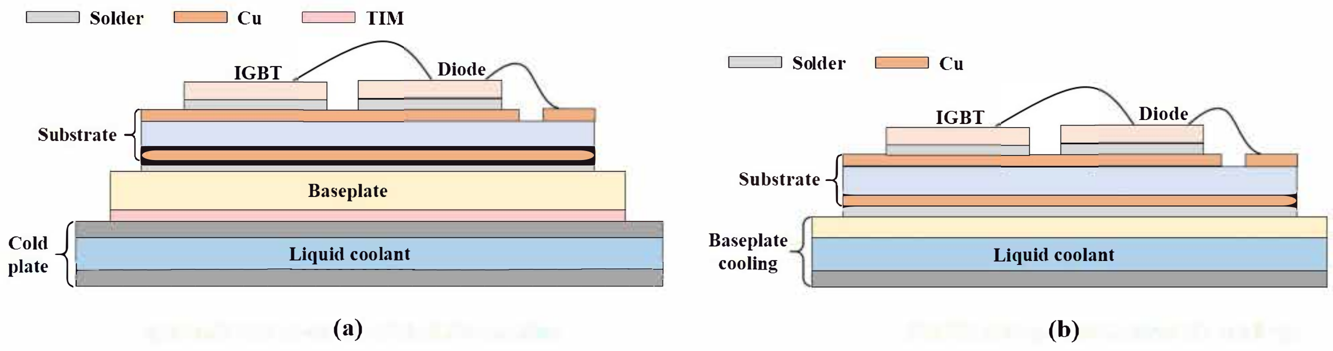

Figure 4. Schematic of (**a**) indirect contact cold plate cooling and (**b**) direct contact baseplate cooling.

Table 5. Summary of studies focusing on indirect contact cold plate cooling.

Reference	Target Devices	Single-Phase/ Two-Phase	Working Fluid	Cooling Device	Cooling Capability	Temperature Control Performance
Vetrovec [55]	HEV inverter	Single-phase	Liquid metal (Ga68.5In21.5Sn10)	Novel active heat sink	>1200 W/cm^2	Temperature fluctuation: <±1 °C
Wang et al. [56]	EV inverter	Two-phase	R134a	Straight microchannel cold plate	Up to 500 W/cm^2	Maximum surface temperature difference: 3.9 °C
Mancin et al. [57]	Avionics	Two-phase	R134a	Straight microchannel cold plate	N/A	N/A
Wang et al. [58]	HEV inverter	Single-phase	Ethylene glycol/water mixture	Straight microchannel cold plate integrated with TEC	200 W/cm^2	N/A
Zhao et al. [59]	HEV inverter	Two-phase	Ethylene glycol/water mixture	Straight microchannel cold plate	250 W/cm^2	N/A
Sakanova et al. [60,61]	Aircraft converter	Single-phase	Water, aviation turbine fuel, and liquid metal (Ga68In20Sn12)	6 pass cold plate with serpentine bends	N/A	N/A
Aranzabal et al. [62]	EV inverter	Two-phase	R134a	Straight channel cold plate	N/A	N/A
Olejniczak et al. [63]	EV inverter	Single-phase	Ethylene glycol/water mixture	Cold plate with pin fin structure	N/A	N/A
Gurpinar et al. [64]	EV inverter	Single-phase	Ethylene glycol/water mixture	Manifold microchannel cold plate in a novel double-side configuration	N/A	N/A
Aranzabal et al. [65]	EV inverter	Two-phase	R134a	Cold plate with two three-column thermosiphons in series	N/A	Reduce maximum gradient temperature from 16 to 10 °C
Mademlis et al. [66]	EV inverter	Single-phase	Ethylene glycol/water mixture	Cold plate with rectangular pin fin structure	N/A	N/A
Ladeinde et al. [67]	Avionics	Single-phase	Air	Cold plate with various folded fins	N/A	N/A
Raske et al. [68]	Avionics	Single-phase	Ethylene glycol/water mixture	Cold plates with either a serpentine channel or a fluid topology-optimized channel	N/A	N/A

2.2.1. Single-Phase Cold Plate

Since the heat dissipation capability of the cold plate is strongly dependent on the cold plate channel configuration, many types of cold plates with different channel structures were developed to improve the thermal performance in the last decades [31,36,63]. Depending on the available exterior surfaces for heat dissipation, a one-sided cooling cold plate or double-sided cooling cold plate can be designed. Figure 5 shows the schematics of three typical single-sided liquid cooling structures (including straight channel structure, serpentine channel structure, and pin fin structure) and one double-sided liquid cooling structure [36]. In general, water–ethylene glycol is used as the coolant in the single-phase liquid cooling system in automobiles, while fuel and polyalphaolefin are usually adopted in the liquid cooling loops of aircraft. In terms of single-sided cooling, the power module is cooled by a cold plate attached to the baseplate through TIM from one side. In contrast, the planar module is sandwiched between two substrates for the double-sided cooling scheme [69]. Note that the wire bonds are required for top connections of components [70]. In this way, heat generated by the power module can be dissipated from both the top and bottom sides, thus enlarging the heat transfer area and increasing the cooling efficiency [71]. Liu et al. [72] developed a SiC automotive inverter using a double-sided cooling scheme. Multiphysics couplings between thermal, electrical, and thermomechanical aspects were numerically simulated to perform the optimization design of the power module. Then, a prototype was also tested. Results showed that the power module with double-sided cooling could further reduce the stray inductance, thermal resistance, and stress in comparison with the one-side cooled modules.

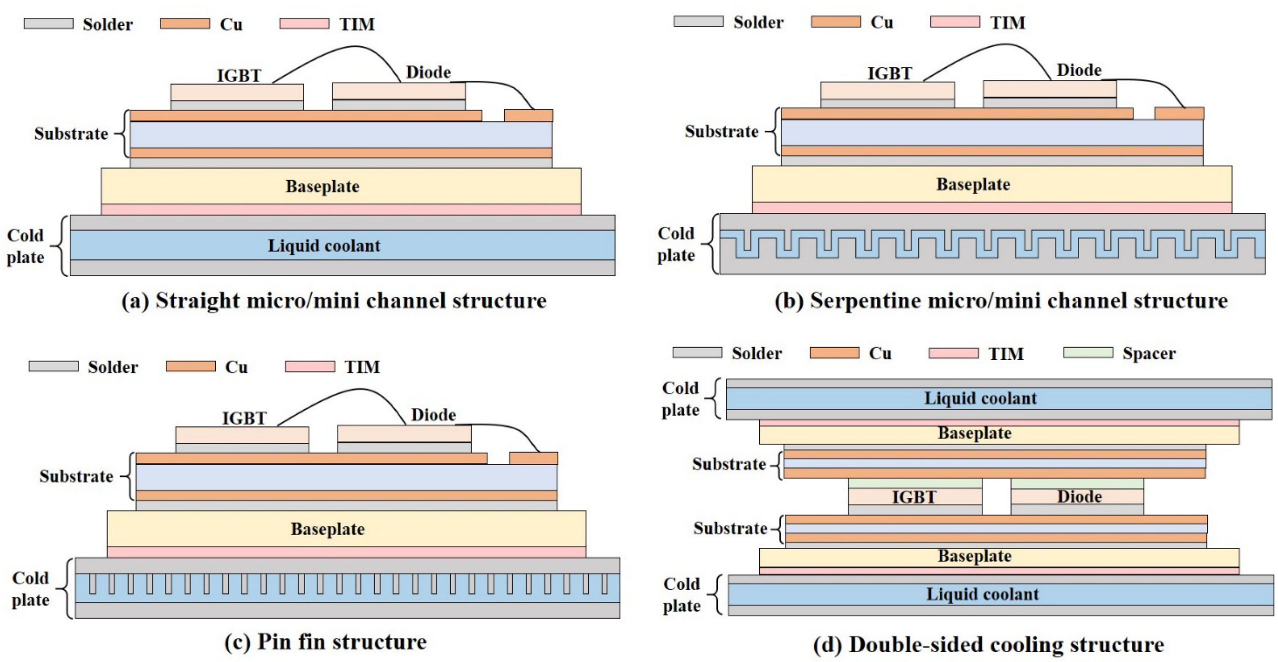

Figure 5. Schematics of different types of cold plate [36].

In the automotive community, when performing the thermal design of the developed power modules, electrical engineers usually adopt a commercially available cold plate according to specific selection criteria [52,53,63]. As a result, overdesign and mismatch between the thermal load of power modules and the cooling capacity commonly exist. Thus, it is essential to perform a dedicated design on the cold plate targeted for a specific power module. Over the last decades, the micro-/minichannel and pin fin structure cold plates have attracted great research interests because of their high heat transfer efficiency and compact size. Becker et al. [73] performed a thermal optimization of a circular pin fin cold plate used for cooling the SiC MOSFET inverter to increase the power density under automotive conditions. Results demonstrated that the thermal coupling of the chips was significantly reduced by increasing the chip distance, resulting in a much more uniform temperature distribution. Gurpinar et al. [64] adopted a manifold microchannel cold plate to provide effective thermal management of SiC MOSFETs for EVs. This cold plate was sandwiched between the two heat sources, as shown in Figure 6. The microchannel side of the heat sink, which exhibited much higher cooling capacity, was used to cool the power module with high heat flux. The coarser macrochannel structure on the manifold side was used to cool the capacitor with relatively lower heat flux. This unique cooling strategy with a sandwiched structure provided a good balance between module compactness and the specific cooling requirements.

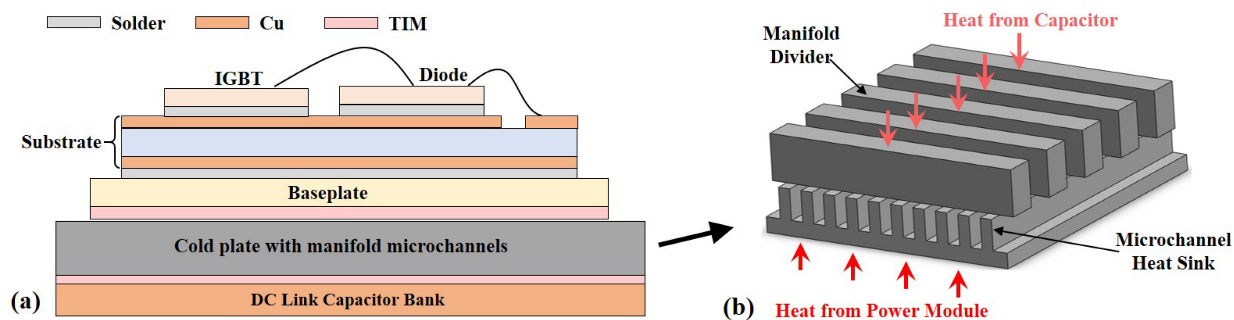

Figure 6. Schematic of (**a**) a cold plate with a sandwiched structure and (**b**) the cooling structure of manifold microchannels [64].

Moreover, the electrical and thermal characteristics of the power modules are strongly related to the performance of the applied cold plate [74]. In this regard, it is extremely necessary to develop the power modules and the corresponding cooling scheme by performing a comprehensive and multidisciplinary optimization. Note that the multidisciplinary optimization for the overall performance improvement also attracts great research interests. Mademlis et al. [66] proposed a multidisciplinary optimization approach based on the accurate electrical, thermal, and fluid mechanics modeling of the design process for a SiC power module under transient load conditions. A pin fin cold plate was initially designed via steady-state numerical simulations, and then was fine-tuned through transient simulation by using the proposed design algorithm. The heat dissipation requirements for the module during both the official driving cycles and the abrupt acceleration tests were considered. Thus, it can not only avoid overheating in all operating conditions, but also provide accurate thermal modeling of individual inverter modules for life estimation and overload capacity calculation. Additionally, the total weight and volume of components should be concerned during the design phase for the TMS in aircraft due to its contribution to the increased operating cost of the aircraft. Figure 7 illustrates a single-phase aircraft TMS [41]. Commonly, the fuel is thought to be the most basic and most important heat sink even for the advanced aircraft, such as F-22 [41,67]. Raske et al. [68] performed a topology optimization over a cold plate for the thermal management of electric parts in aircraft engines. The performance of the topology-optimized design and that of the traditional serpentine channel cold plate were compared. Results indicated that the peak temperature for the optimized case was 4 °C lower, and a mass reduction of 38.5% could also be obtained.

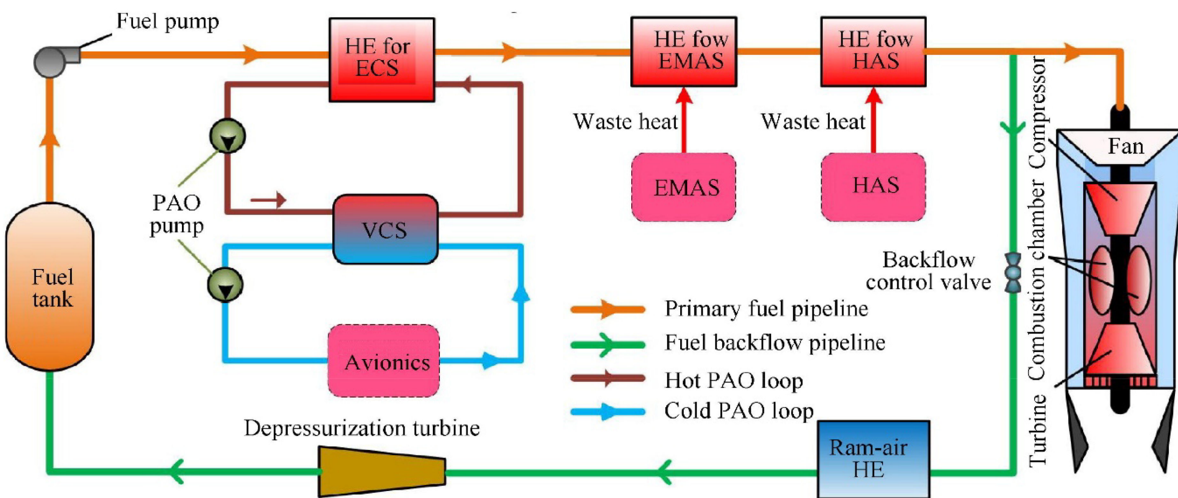

Figure 7. Layout of a single-phase MPFL system in aircraft [41].

For further exploring the potential performance improvement of TMS from the perspective of working fluid, Sakanova et al. [61] investigated the weight contribution of the single-phase cold plate cooling system for the power electronics on board aircraft. The cooling systems with different working fluids, including the fuel and water, were compared. Results indicated that the fuel could satisfy the cooling demand while providing the least pressure drop. Then, they further investigated the contribution of the cooling system to the total weight when using liquid metal as a coolant in the cold plate [60]. Different types of coolant were compared, including the fuel, water, and gallium alloy (Ga68In20Sn12). It was indicated that the cooling system could be much lighter while keeping a similar thermal performance if the liquid metal was used as a coolant. For example, the typically used pump could be replaced by a 12-times-lighter pump in the cooling system. Similarly, a novel cooling scheme using liquid metal rather than the commonly adopted water–ethylene glycol engine coolant was developed for the thermal management of HEV inverters due to its relatively low freezing point, low kinematic viscosity, high thermal conductivity, and excellent wetting properties [55].

Some efforts were also taken to enhance the cooling capacity via the endothermic chemical reaction, such as thermal cracking of the aircraft fuel [75]. Wang et al. [41] summarized in detail research efforts to augment the cooling capacity of the fuel-based TMS. Their study mainly focused on the thermal cracking characteristics and associated effects of the fuel decomposition process and heat transfer characteristics of aviation kerosene under the supercritical conditions and so on. Since thermal cracking is not selective and several competitive exothermic reactions may occur, catalytic cracking is thought to be more suitable than thermal cracking for heat sink enhancement of the fuel-based TMS. However, the aforementioned technology was not applied in practical applications due to reliability concern. It should be mentioned that a small temperature gradient over the target electronics is preferred because the stresses and potential failure induced by the large temperature gradient can greatly raise the reliability risk. Wang et al. [58] proposed a hybrid cooling system design, which combined cold plate liquid cooling and a TEC device for highly effective cooling of an HEV inverter. A cold plate was used for global cooling of the entire module, while a thin-film TEC was embedded in the module for the isothermalization of the individual IGBT chip. Results indicated that this hybrid cooling scheme could substantially improve the uniformity of the IGBT chips. In this regard, a nonuniform temperature distribution usually presents in the electronics surface when implementing the single-phase cold plate cooling method. Moreover, the parabolic-like temperature profile cannot be effectively suppressed by simply improving the cooling capacity of cold plates. From the viewpoints of electrical design and device reliability, it is highly desirable to maintain the surface temperature of the devices as uniformly as possible. In this regard, the combination of cold plates with other thermal management techniques may achieve a favorable performance.

2.2.2. Two-Phase Cold Plate

As previously mentioned, the single-phase TMS exhibits relatively lower cooling capacity and poor uniformity. To satisfy the dramatically increasing heat flux, a two-phase cold plate, where the liquid-to-vapor phase transition occurs, is identified as a very promising high heat flux cooling solution [76]. Compared with the single-phase cold plate, the two-phase cold plate can provide much higher heat transfer efficiency, more uniform temperature distribution, and lower pumping power at lower flow rates. Besides, the performance and reliability of the power electronics can be substantially improved. Commonly, the two-phase cooling system is based on conventional automotive air-conditioning systems with a cold plate serving as the evaporator [65]. The integration of a miniature vapor compression cycle allows the working medium evaporating inside the cold plate and the heat release to ambient under higher temperature difference. The performance of a single-phase and that of a two-phase cold plate used for the Toyota Prius motor inverter was compared by Wang et al. [56] via first-order analysis and system-level simulations. Compared with the single-phase cold plate, the two-phase cold plate using R134a as coolant could greatly reduce the peak device temperature with very uniform temperature distribution and lower the pumping power by using the same cold plate. Thus, the two-phase cold plate presented great potential due to its low-cost, small-volume, and high-performance cooling scheme, which can pronouncedly improve the system reliability and conversion efficiency of vehicle inverters. Aranzabal et al. [62] investigated the two-phase cold plate for EV power module thermal management and compared its performance with that of a single-phase cold plate. Results indicated that the two-phase cooling with the refrigerant R134a could provide much better cooling performance by consuming lower pumping energy. Besides, a maximum temperature gradient of 40.6 °C among the chips was produced for the single-phase cooling, while this value could be reduced to 16.1 °C at the same conditions. Moreover, it was also found that the application of two-phase cooling can alleviate the thermal environment of the motor inverter from the perspective of both system reliability and conversion efficiency. However, for the two-phase cooling technologies, some major concerns still exist, which need further in-depth investigations. For example,

the two-phase flow instability in the microchannels may result in pressure fluctuations, electronics overtemperature, and even device failure. Zhao et al. [59] proposed a novel cooling technology by using subcooled boiling in microchannels to reduce the junction temperature of automotive power electronics. Numerical studies were performed to verify the feasibility and demonstrate its great advantages. It was found that 25% more heat could be removed from the power electronics via the subcooled boiling in comparison with the conventional single-phase forced convection cooling scheme. Besides, this cooling scheme could also achieve electronics operating under the junction temperature at a lower coolant flow rate, simplify the cooling system, and reduce the weight and cost of HEVs.

When applying the two-phase cold plates to the aircraft electronics cooling, particular attention should also be paid to the cold plate design to meet the volume and size limitations of the aeronautical standards. Mancin et al. [57] experimentally studied a miniature vapor compression cycle TMS equipped with a cold plate for aeronautical electronics cooling. R134a was used as a working fluid, and a new oil-free linear compressor was developed for the miniature refrigeration system. The measured temperature profile of the cold plate highlighted the presence of the vaporization regions, which could be generally divided into three parts: a two-phase heat transfer region, a dryout region, and a postdryout region. In terms of the two-phase heat transfer region, the wall temperature remained almost constant because of the stable vaporization of the coolant. In the dryout region, the wall temperature increased suddenly. Then, the temperature remained almost constant again in the postdryout region. The preliminary results showed that the thermal behavior and safe operation of the system could be deeply affected by the dryout phenomenon. Hence, further investigations on the two-phase cold plate are needed to obtain in-depth knowledge on the two-phase operating characteristics to predict the critical conditions. In addition to the mass and size consideration discussed above, the safety, stability, and controllability should also be given great importance. Moreover, for the next-generation military aircraft, highly transient thermal loads that exceed the cooling capacity of current aircraft TMSs need to be handled. Accordingly, the reliable control becomes a significant challenge when applying the active vapor compression cycle thermal management method. The control of the conventional vapor compression cycle is achieved by using proportional–integral controllers in a separate single-input single-output control loop. This simple method succeeds when the thermal mass of the system is large and the loads change slowly. However, the system greatly suffers an unsteady process due to the highly transient loads, even experiencing unstable risk in some cases. To achieve a reliable control to the system, Jackson et al. [77] designed a linear quadratic regulator for a simple vapor compression cycle system. Result showed that the linear quadratic controller significantly outperformed the traditional proportional–integral controller, which was regarded as the basic case.

2.3. Direct Contact Baseplate Cooling

The direct contact baseplate cooling structure is shown in Figure 4b, which is much more promising because of its higher heat transfer performance, more compact size, and lighter weight compared with the commonly used indirect contact cold plate cooling method. The baseplate and heat sink are typically integrated into one component to enable the direct contact between the baseplate and coolant [51]. As a result, the extra TIMs and heat spreaders could be eliminated, and the heat transfer path is shortened accordingly. It was proposed that the nonuniform temperature distribution of the baseplate is the drawback of the baseplate cooling method dependent on the fluid channel structure [78]. Nonneman et al. [79] performed a comprehensive comparison of different cooling methods for a typical inverter of AEVs, including the forced air cooling, forced air cooling with embedded heat pipes, forced air cooling with a vapor chamber, conventional indirect contact cold plate, direct contact baseplate and pin fin cooling, and two-phase immersion cooling. Results showed that the case where pin fins were integrated in the baseplate always presented the best overall performance. Wang et al. [80] also developed a baseplate cooling system prototype with pin fins integrated to the baseplate of the module for a DC/AC

powertrain system of AEVs. The performance of the cooling structure was compared with that of an indirect contact cold plate cooling structure. It was found that the thermal resistance could be reduced by more than 50% by applying the direct baseplate cooling method. Meanwhile, the thermal grease layer was eliminated. Besides, both active and passive temperature swings decreased significantly, thus improving the module reliability and lifetime. The lifetime of the modules using both a conventional and integrated liquid cooling scheme was also estimated under standard driving cycle tests. Results indicated that the lifetime was significantly prolonged by applying the direct baseplate cooling with pin fins. Similar to the indirect contact cold plate cooling method in a prior section, the direct contact baseplate cooling can also be categorized into single-phase and two-phase schemes. Table 6 summarizes studies focusing on the direct contact baseplate cooling.

Table 6. Summary of studies focusing on the direct contact baseplate cooling.

Reference	Target Devices	Single-Phase/ Two-Phase	Working Fluid	Cooling Device	Cooling Capability	Temperature Control Performance
Xu et al. [81]	HEV inverter	Single-phase	Ethylene glycol/water mixture	Integrated baseplate with pin fin structure	N/A	N/A
Wang et al. [80]	EV inverter	Single-phase	Ethylene glycol/water mixture	Integrated baseplate with circular pin fin structure	N/A	N/A
Jung et al. [82]	EV inverter	Two-phase	R245fa	Embedded microchannels with a 3D manifold	Up to 1000 W/cm^2	N/A
Uhlemann et al. [83]	HEV inverter	Single-phase	Ethylene glycol/water mixture	Flat baseplates with ribbon bonded cooling structures	N/A	N/A
Jung et al. [84]	HEV inverter	Single-phase	Water	Embedded silicon microchannel baseplate with a 3-D liquid distribution manifold	250 W/cm^2	Maintain a maximum chip temperature of 90 °C
Hou et al. [85]	HEV inverter	Two-phase	R134a	Integrated baseplate with a plate fin structure	380 W/cm^2	Maintain the chip temperature at about 90 °C
Hou et al. [86]	HEV inverter	Two-phase	R1234yf	Integrated baseplate with a plate fin structure	>500 W/cm^2	Maintain the chip temperature below 120 °C
Yuki et al. [87]	EV inverter	Two-phase	Distilled water	Baseplate with lotus copper	>500 W/cm^2	N/A
Shi et al. [88]	Inverter	Single-phase	Water	Microchannel baseplate with longitudinal vortex generators	N/A	N/A

2.3.1. Single-Phase Baseplate Cooling

Xu et al. [81,89] developed a 30 kW Si-based automotive inverter using direct baseplate cooling with a pin fin structure for operation with the 105 °C engine coolant, as shown in Figure 8a. The water–ethylene glycol engine coolant at a high temperature of 105 °C was used for cooling the power semiconductor devices. Experimental results demonstrated that the power module can operate continuously with the 105 °C high temperature coolant without sacrificing efficiency. Similarly, Becker et al. [73] performed a thermal optimization for a three-phase SiC MOSFET automotive inverter assembly with circular pin fins. The thermal coupling of the chips was significantly reduced by increasing the chip distance, leading to a more uniform temperature and, therefore, current distribution between the chips of one switch. However, existing pin fin solutions suffer from low design flexibility and high production and material costs. Then, Uhlemann et al. [83] further designed a novel flat baseplate with a ribbon bonded cooling structure, which can be seen in Figure 8b. The ribbon bonded cooling structures were placed on a nickel plated flat baseplate using a bond pattern with an optimized thermal design. This new cooling concept was characterized by good design flexibility, high-cost effectiveness, and excellent thermal performance.

Jung et al. [82] compared the thermal resistance and pressure drop of three different microchannel cooling structures, including the traditional attached heat sink, embedded baseplate cooling, and embedded baseplate cooling with 3D manifold. Results indicated that the embedded baseplate cooling with a 3D manifold architecture exhibited greatly reduced thermal resistance in comparison with other cooling components. Then, they

further investigated the embedded silicon microchannel baseplate with 3D liquid distribution manifolds and vapor extraction conduits for HEVs' power electronics [84]. Figure 9 depicts the conceptual design of the embedded Si/SiC microchannel baseplate with a 3D manifold structure. The manifold was made of Si and then bonded to a Si-based microchannel substrate to form a monolithic microcooler. Experimental results demonstrated that the embedded microchannel-3D manifold cooling structure was capable of removing 250 W/cm^2 heat flux while maintaining the maximum chip temperature below 90 °C. Moreover, numerical simulation results also hinted the possibility of removing heat flux up to 850 W/cm^2 at a maximum chip temperature of 166 °C by using water as a coolant. Recently, Shi et al. [88] developed two different microchannel designs for the baseplate cooling of the IGBT module. The thermal hydraulic performance was compared via numerical simulations. Compared with the longitudinal counterflow scheme, a much better heat transfer performance and smaller pressure can be obtained by using the horizontal counterflow scheme. Besides, longitudinal vortex generators were also introduced in the horizontal counterflow microchannel to further heat transfer enhancement.

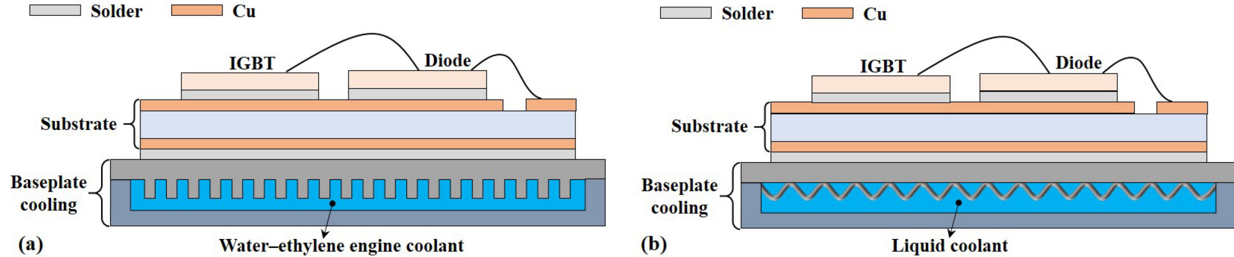

Figure 8. Schematic of (**a**) the conventional baseplate cooling with a pin fin structure and (**b**) the novel directly cooled HybridPACK^{TM} power modules with ribbon bonded cooling structures [81,83].

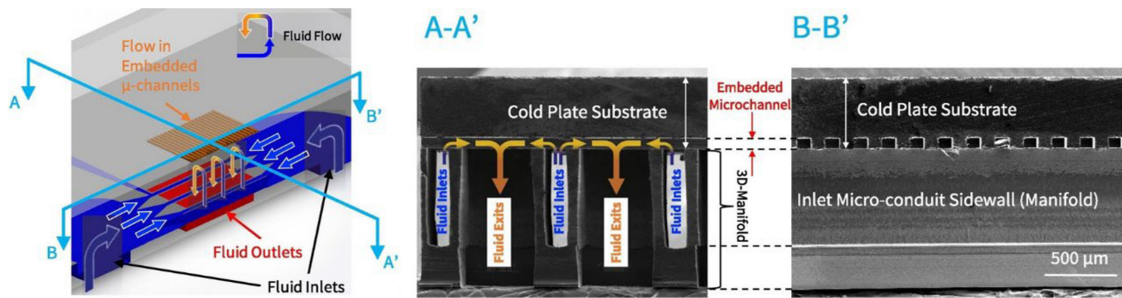

Figure 9. Conceptual design of the embedded Si/SiC microchannel cooling with a 3D manifold structure [84].

2.3.2. Two-Phase Baseplate Cooling

In the future automotive inverter system, the implementation of SiC-based electronics will enable engineers to apply a high-temperature (up to 110 °C) coolant for thermal management, thus eliminating the additional low-temperature cooling fluid loop. To provide efficient thermal management for automotive inverters with heat flux up to 500 W/cm^2, Yuki et al. [87] proposed a breakthrough stacking structure without a heat spreader. The direct cooling method via two-phase immersion was experimentally verified in a saturated pool boiling environment. The lotus copper was jointed onto a grooved surface to spontaneously induce the breathing phenomenon. The critical heat flux (CHF) could be obtained as high as 500 W/cm^2. This new concept may provide viable guidance in the structure design of novel TMS. Since this is a fundamental test over the new cooling scheme, research works upon the mechanism clarification and accurate thermal management control still require further investigations. Hou et al. [85] investigated a plate fin evaporator in a compact two-phase cooling system with R134a as a working fluid. The cooling performance was evaluated by packaging the Si-based thermal test vehicles in the

center cavity of a substrate. Results indicated that a heat flux over 380 W/cm^2 could be dissipated while maintaining its temperature at about 90 °C. Then, they further investigated this two-phase microchannel TMS for power electronics over 500 W/cm^2 heat dissipation. An environment-friendly refrigerant with low boiling points, R1234yf, was selected as a working fluid. The experimental results showed that the TMS could dissipate a heat flux of 526 W/cm^2 while maintaining the junction temperature below 120 °C. Moreover, for SiC-based power electronics with a higher junction temperature, this system was expected to dissipate a heat flux up to 750 W/cm^2 [86]. Recently, T'Jollyn et al. [90] experimentally investigated the heat transfer performance of the baseplate via pool boiling. Especially, a refrigerant with lower global warming potential, FK-649, was used as a coolant to achieve a higher heat dissipation efficiency.

2.4. Jet Impingement Cooling

Jet impingement cooling has been widely adopted for thermal management in various industrial applications because of its prominent capability of dissipating large heat flux. However, it has not been implemented in marketed vehicles and aircraft [91–93]. Figure 10a shows a schematic of a jet impingement cooling power inverter module. Jones-Jackson et al. [37] reviewed the state-of-the-art jet impingement designs and future jet impingement technology applied for power electronics cooling. Advanced jet impingement cooling technology developed for EV power modules was outlined. It was pointed out that while a large amount of studies on jet impingement had been performed, further investigations were required for automotive applications specifically. Ekkad et al. [94] investigated the performance of a mini jet impingement scheme and a ribbed mini channel cold plate for cooling the PCU of HEVs. A parametrical study was performed to obtain the best-performing structure. It was indicated that the thermal performance was significantly improved by applying the jet impingement at the expense of an increased pressure drop in comparison with a minichannel cold plate. Then, a ribbed minichannel cold plate was further investigated to improve the thermal performance without significantly increasing the pressure drop. The ribbed minichannel cold plate could apparently improve the average heat transfer coefficient at the target surface with a much smaller pressure drop. Similarly, Gould et al. [95] designed a jet impingement cooling system for cooling the baseplate of a SiC-based power module in military HEV applications. The device was cooled using a 100 °C water–ethylene glycol coolant with an ambient air temperature of 120 °C. Compared with the commercial off-the-shelf cold plate and the microchannel cold plate, the heat dissipation capability of the module using jet impingement cooling increased by 2.5 and 1.5 times, respectively.

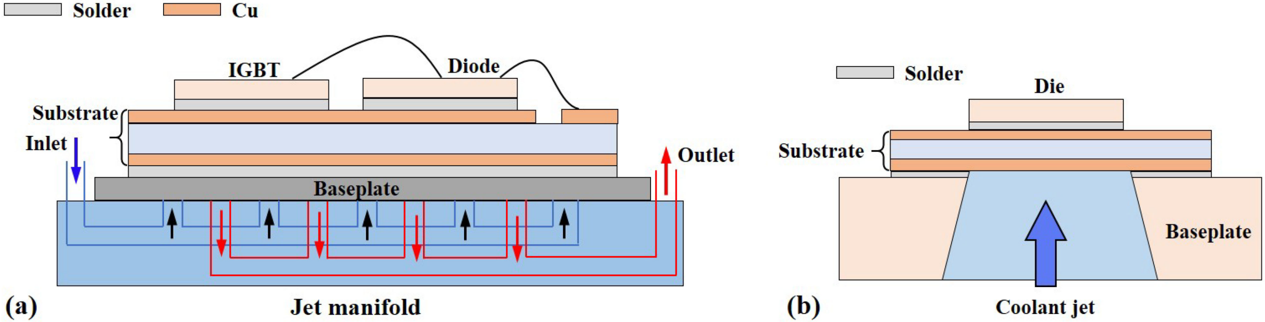

Figure 10. Schematic of (**a**) the power module with multijet impingement cooling and (**b**) the direct backside jet impingement cooling [37,42].

When applying the jet impingement cooling scheme for inverters, the overall thermal resistance of the module can be further reduced by shortening the heat transfer path. For example, holes are cut through the baseplate all the way to the backside of the DBC substrate, and nozzles are positioned under the DBC with coolant jets impinging on the backside, as shown in Figure 10b [42]. As a matter of fact, this method is thought to be

a very promising cooling option for automotive power electronics with high heat flux in the near future. Bhunia et al. [96] developed a close-loop jet impingement cooling system for thermal management of an automotive inverter. A jet array with an antifreeze liquid at an inlet temperature of 105 °C was designed to directly impinge on the baseplate of the module. Results demonstrated that a heat dissipation capacity of 1623 W was obtained for a 20 °C device temperature rise above the ambient, indicating approximately 1.8 times improvement over the commonly used single-phase forced liquid cooling with a pin fin cold plate. Tang et al. [97] proposed a SiC-based power module with integrated temperature sensors using the dual-side liquid cooling via jet impingement. The cooling performance of this liquid cooling system was improved by optimizing the flow channel width, nozzle length, and jet to wall distance. However, this cooling method suffers great pressure drop, which severely restrains its application. Moreno et al. [98] developed a novel TMS for automotive power electronics by combining slot jets impinging on finned surfaces and a low-thermal-resistance package, which eliminated metalized ceramic substrates. A dielectric fluid was adopted as a coolant to allow direct cooling of electrical components.

To further improve the heat transfer performance and reduce the operating temperature of the power module, Pourfattah et al. [99] proposed a novel cooling system by combining the jet impinging with the pin fins and vortex generators. Moreover, the thermal hydraulic performance was numerically evaluated and further optimized by employing the response surface method and genetic algorithm. It was found that a uniform temperature distribution could be obtained at the optimum point, and the peak temperatures of the IGBT and diode were 75 and 58.8 °C, respectively. Moreover, multiphysics optimization based on the coupling of the electrical and thermal aspects of a converter in EVs was also required to meet the stringent comprehensive performance requirements. Zaman et al. [100] performed a multidisciplinary optimization of a jet impingement cooling system in automotive applications by applying the genetic algorithms to generate topologically optimized geometries. Note that most of the studies focusing on the jet impingement cooling system for vehicles are based on the steady-state analysis. It is not adequate and accurate to perform a comprehensive performance evaluation when considering the practical application in a vehicle. Recently, Jones-Jackson et al. [101] compared the cooling performance of a conventional pin fin baseplate and a flat plate jet impingement cooling system at both steady and transient simulations. Results demonstrated that the jet impingement cooling could greatly reduce the junction temperature and improve the temperature uniformity of the power module. In addition, the jet impingement system was capable of ensuring the MOSFET and diode junction temperatures within the safe operating range throughout the entire drive cycle.

2.5. Spray Cooling

In addition to the jet impingement cooling, the spray cooling is also regarded as a viable alternative for future automobile and aircraft platforms [102]. Different from jet impingement where the fluid is ejected as a stream, the spray cooling utilizes the momentum of liquid emanated from the nozzle to induce fine droplets to individually impinge upon the target surface [17,103,104].

In the early times, efforts were taken to demonstrate the viability and assess the cooling performance of various spray cooling strategies for automotive power electronics. Figure 11 shows a schematic of a typical spray-cooled inverter module [105]. Mertens et al. [106] compared the performance of three cooling methods, including the single-phase convection with water, spray cooling with either air–water or steam–water. Experimental results indicated that the air–water spray cooling exhibited superior cooling performance over other two cooling methods. The National Renewable Energy Laboratory of the U.S. Department of Energy also explored the viability and implementation of spray cooling as next-generation cooling solutions for HEV electronics [107]. According to the assessment of various commercial coolants, HFE-7100 was identified as the optimum coolant in terms of thermal, environmental, safety concerns and material compatibility. Besides, the desired ranges of spray parameters were identified to safely remove a heat flux of 150–200 W/cm^2

while maintaining the electronics temperature below 125 °C. Turek et al. [108] experimentally investigated a pressure-atomized evaporative spray cooling nozzle array for an inverter module. The water–propylene glycol antifreeze coolant at a temperature of 100 °C was used as a coolant. The sprays impinged directly onto the backside of the DBC substrate to reduce the thermal resistance. Results indicated that the IGBT module could safely operate at a heat flux up to 140 W/cm^2 while maintaining the junction temperature below 125 °C. Then, they also tested the spray cooling system with 95 °C water as a coolant for thermal management of hybrid propulsion systems of aircraft. It was found that the temperature of IGBT cooled by a water spray was about 10 °C lower than the water–propylene glycol mixture [109]. Recently, Siddiqui et al. [110] investigated the spray residue surface effects of the hybrid nanofluid on the spray cooling performance. Compared with the water spray cooling, the CHF was enhanced up to 126% when using the hybrid nanofluid spray cooling. This was mainly due to the high latent heat of vaporization and the wetting and wicking effects of the residue. Moreover, the hybrid nanofluid spray cooling potential was assessed to address heat dissipation issues for HEV/AEV high-power electronics. Results indicated that the power electronics used for current and future EVs could be kept below their failure temperatures by applying the hybrid nanofluid spray cooling, which cannot be achieved by using either water or a dielectric fluid as a coolant.

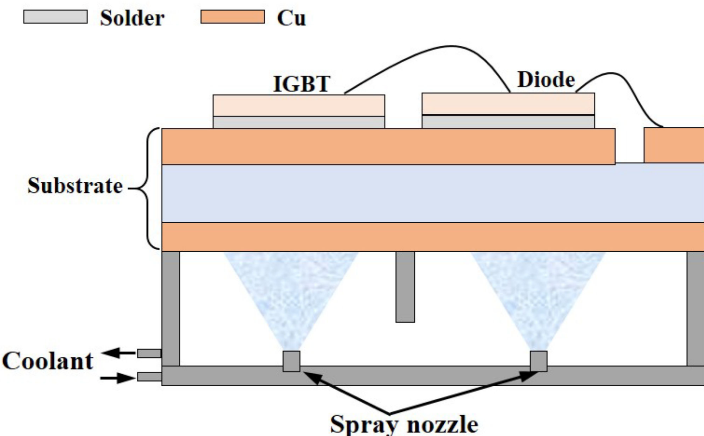

Figure 11. Schematic of a typical spray-cooled inverter module [105].

In addition to the coolant, the cooling surface can also fundamentally affect the liquid–wall interactions and the heat transfer performance in spray cooling. In this regard, improvement on surface properties and structures is considered very promising approaches to enhance spray cooling. Bostanci et al. [105] developed a spray cooling system for the thermal management of an automotive inverter. An array of 1 × 2 pressure atomized nozzles was applied in the system using a 90 °C antifreeze coolant. An enhanced microstructured spray surface with protrusions at an average roughness of 15–16 µm was fabricated to enhance the heat transfer. Results showed that a heat flux of up to 400 W/cm^2 could be obtained with only 14 °C surface superheat. Then, they further evaluated the reliability of the spray cooling for long-term operation with up to 2000 h under a constant heat flux of 200 W/cm^2 [111]. A very consistent device temperature (within ±1.3 °C) could be obtained throughout the testing period. Recently, they experimentally compared the spray cooling performance of three enhanced surfaces using HFC-134a and HFO-1234yf refrigerants as coolants [112]. Results indicated that HFC-134a can provide better cooling performance in comparison with HFO1234yf mainly due to the thermophysical property differences. Besides, the electroplated microporous surface exhibited the highest heat transfer performance among the tested surfaces. However, there is no consensus on the principles to guide the design of engineered surfaces when surface-enhanced spray cooling is used [113].

During the practical operation, the power loss of automotive electronics usually varies within the driving cycle. In this regard, an intelligently dynamic thermal management may

be more advantageous. Panão et al. [114] designed an intermittent multijet spray cooling system, which was able to efficiently respond to power peaks. The spray intermittency was dependent on the duration and frequency of injection. The maximum heat flux removal was obtained while stably maintaining the surface temperature below 125 °C. Compared with the continuous spray mode, the intermittent spray allowed benefiting more from the phase-change convection process.

To examine the potential of an airborne spray cooling system, Xu et al. [115] evaluated various typical cooling methods for high heat flux dissipation and reviewed the advancement of spray cooling technology. Generally, due to infancy studies on the air-oriented spray cooling technologies, there is still a lack in the knowledge of the unique heat transfer behaviors and flow patterns resulting from the complicated operating environments [116]. Venkategowda et al. [117] explored the potential of the evaporative spray cooling for MEA avionics. Both single-phase sub-boiling and two-phase nucleate cooling were considered. The sensitivity of the heat dissipation capability to the coolant with a variable Reynolds number and ratio of the heating plate diameter to the nozzle diameter of the spray cooling system was analyzed. Moreover, for aircraft, especially the military aircraft, abrupt acceleration and changes in gravity may bring significant trouble in the application of the spraying cooling system [41,118]. More detailed information will be discussed in Section 4.

3. Passive Methods

3.1. Heat Pipes

Due to the prominent advantages of passive operation, reliable design, cheap cost, and superior performance, heat pipes are widely adopted for electronics cooling [119,120]. Not only the efficient heat transfer capability, but also a relatively uniform temperature distribution can be obtained via the utilization of heat pipes. As summarized in Table 7, various types of heat pipes have been developed for cooling heat generation sections on automobiles and aircraft, such as the flat heat pipes, pulsating heat pipes (PHPs), and loop heat pipes (LHPs) [28,119,121].

Table 7. Summary of heat pipes used for thermal management of electronics on board automobiles and aircraft.

Reference	Target Device	Types of Heat Pipes	Heat Transfer Fluid	Objective
Zaghdoudi et al. [122]	Avionics electronic modules	Mini flat heat pipe	Water	Eliminate hot spots and spread the heat dissipated from the components.
Cai et al. [123]	High-power electronic devices in avionics systems	PHP	Water	Construct a quick heat transfer path from the electronic devices to the external heat sink.
Singh et al. [124]	Automotive dashboard that is heated by radiative heat transfer from the engine	Capillary pumped loop	Acetone	Thermal management of up to 210 W at the source and heat transfer over 1 m.
Anderson et al. [125]	Avionics in high-temperature environments	LHP with multiple condenser	N/A	Improve the heat transfer efficiency within electronics enclosure and identify potential sinks to provide continuous heat rejection over the operating envelope of the platform.
Reyes et al. [126]	Avionics modules	Vapor chamber	HFE 7100	Function as a heat spreader.
Burban et al. [127]	HEV power electronics	PHP	Acetone, methanol, water, n-pentane	Heat dissipation of the electronics on board vehicle.
Ellis et al. [15]	Avionics in high-temperature environments	LHP with two condensers	Methanol	Cool the fuel prior to entering the avionics enclosure, which was determined to be more reliable than cooling the avionics directly.
Jones et al. [128]	Avionics modules	Vapor chamber	Water	Reduce the thermal resistance between the avionics component and module heat exchanger.
Cai et al. [129]	Avionics modules	LHP combined with PHP	Water	LHP is developed to transport heat from the avionics chassis to the remote heat rejection site. PHP is developed for heat transfer enhancement.

Table 7. *Cont.*

Reference	Target Device	Types of Heat Pipes	Heat Transfer Fluid	Objective
Tecchio et al. [130]	Avionics modules	One heat pipe combined with four thermosyphons	Water	Provide passive cooling for electric-powered equipment installed in aircraft.
Zilio et al. [131]	Integrated modular avionics in helicopters	LHP	Water	Eliminate hot spots at the blade level.
Accorinti et al. [132]	Converter onboard hybrid propulsion aircraft	Capillary pumped loop	Methanol	Ensure a constant operating temperature during the entire mission of the aircraft.
Chen and Li et al. [133–135]	EV inverter	Vapor chamber	Water	Reduce thermal resistance and improve temperature uniformity.
Junior et al. [136]	Avionics modules	Flat thermosyphon	Water	Improve the heat removal efficiency from electronic enclosures.
Vieira et al. [137]	Avionics modules	Loop thermosyphon	Water	Remove heat from airplane electronic equipment boxes.
Pagnoni et al. [138]	Aircraft engine equipment	LHP	Water	Enhance the heat transfer capabilities of currently adopted monophasic solutions.
Dreiling et al. [139]	EV inverter	PHP	N/A	Transfer heat to remote heat sinks.
Singh et al. [140]	Electronics on board EVs	LHP	Water	Eliminate hot spots and transport heat over longer distances.

3.1.1. Flat Heat Pipe

Due to the unique configuration of the flat heat pipe, it is often adopted to serve as a heat spreader for uniform cooling. Zaghdoudi et al. [122] studied the performance of a mini copper–water flat heat pipe that was integrated into an avionics electronic module to reduce the thermal resistance from PCBs to the module wall. Results showed that heat could be removed very well, and the hot spots of the components could be successfully eliminated. Chen et al. [133,134] developed a novel vapor chamber to reduce the thermal resistance and improve the temperature uniformity of IGBT power modules. Different from a traditional package scheme, the baseplate and TIM were not implemented, and the DBC substrate was directly soldered on the lid of a vapor chamber. Besides, a water-cooled plate was bolted to the vapor chamber together with an IGBT power module. The effects of the vapor chamber on the temperature profile, thermal stress, and lifetime of the power module were numerically studied via the finite element method. Results indicated that the thermal and thermomechanical performances of IGBT integrated with the vapor chamber were significantly improved in comparison with that integrated with a copper baseplate. Recently, Li et al. [135] developed a novel one-piece vapor chamber integrated as a baseplate for SiC-based MOSFETs in HEV/AEV applications, which can be seen in Figure 12. By replacing the traditional copper baseplate with a vapor chamber, the overall thermal resistance from junctions to a coolant could be significantly reduced. Besides, a more uniform temperature distribution with a temperature difference across the whole bonding interfaces of 1.4 °C could be achieved. Moreover, the wick design using sintered powder could perform better than the groove and mesh designs in high heat flux applications.

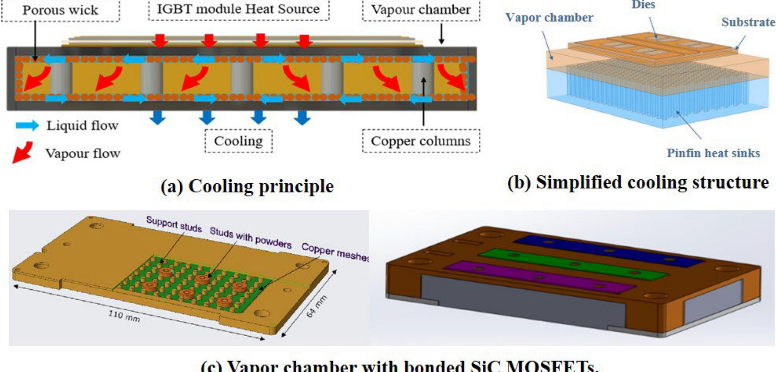

Figure 12. Schematic of the vapor chamber with bonded substrates [135].

Reyes et al. [126] developed a vertically placed vapor chamber-based heat spreader for avionics cooling. A minievaporator area made up of an array of mini–pin fins was implemented to enhance the boiling process inside the vapor chamber. The vapor chamber was found to be much more efficient than an equivalent metallic heat sink that occupied the same volume. For a component surface temperature ranging from 80 to 100 °C, the maximum dissipated power varied between 95 and 145 W. Similarly, Jones et al. [128] embedded the vapor chamber within the avionics module chassis to reduce the thermal resistance between the avionics components and the module heat exchanger. The isothermalization of the avionics baseplate was significantly improved. However, the performance improvements decreased as the number of heat sources increased. Figure 13 illustrates a novel flat thermosyphon developed for avionics cooling [136]. In general, this thermosyphon was similar to a vertically placed vapor chamber. Different from the traditional flat heat pipes operating in vertical orientation, an intermediate plate was implemented in the thermosyphon to divide the device into two connected sections. In this way, the working fluid circulation inside the device could be improved, thus ensuring more efficient operation. Furthermore, on the inner surface of the evaporator plate, a wick medium with five layers of a screen wire mesh was added to suppress liquid accumulation on the bottom side of the flat thermosyphon. In addition, the working fluid at the inner surface of the evaporator could be replenished via the capillary force of the wick medium.

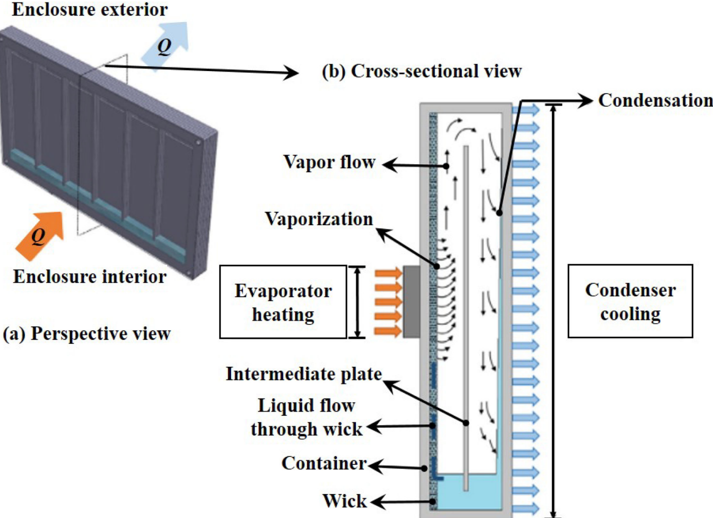

Figure 13. A novel flat thermosyphon and its working principle [136].

3.1.2. Pulsating Heat Pipe (PHP)

Moreover, the PHPs are also adopted for the electronics cooling of automobiles due to their high reliability and reproducibility. A PHP consists of a single plain capillary-sized tube with many U-turns. Heat is absorbed at one end of this tube bundle and then is transported to the other end via a complex pulsating action of the liquid–vapor/bubble–slug system. Cai et al. [123] experimentally investigated the thermal performance of a PHP-based cooling system in avionics applications. PHPs with a 1.65 mm internal diameter were assembled with PCBs onto the avionics chassis. In this way, a quick heat transfer path from the electronics to the external heat sink was constructed, thus enhancing the heat transfer. Experimental results indicated that PHPs were capable of handling long-distance and high-power heat transfer for new-generation avionics systems. Besides, a more uniform temperature distribution could be achieved in comparison with the conventional cooling system. Besides, the evaporator temperature fluctuations were reduced to a reasonable range to ensure a highly efficient operation of electronics. Similarly, Dreiling et al. [139] developed a novel power module integrating a flat-plate PHP into a DBC substrate for automotive and electric aircraft propulsion systems. Tests results demonstrated that the integration of the flat-plate PHP into the substrate structure of power

modules enabled the utilization of remote heat sinks, thus improving the heat transfer efficiency. Burban et al. [127] developed a PHP for electronic thermal management in HEVs. A specific test bench was built to replicate the vehicle environment. The PHP was made of a single 2.5 mm inner diameter copper tube with 16 turns, as shown in Figure 14. To characterize this PHP, four working fluids, including the water, methanol, n-pentane, and acetone, were tested at the thermal power ranging from 25 to 550 W. Besides, three inclinations were also tested to verify its antigravity ability. It was tested that the PHP always worked with satisfactory reliability and reproducibility.

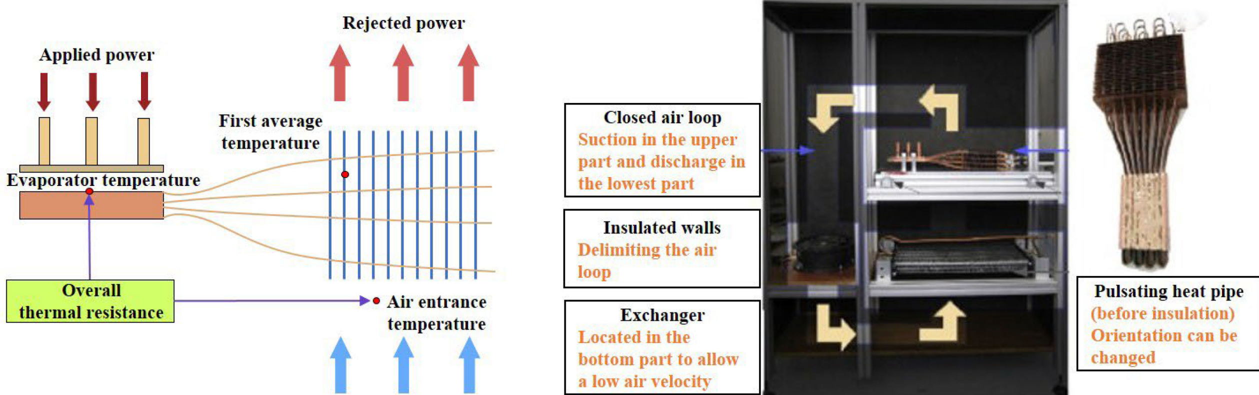

Figure 14. Schematic of the PHP for HEVs and the experimental apparatus loop [123,127].

3.1.3. Loop Heat Pipe (LHP)

LHPs, featuring good properties of transferring considerable heat flux for long distances, have been widely implemented as a heat transfer device [141]. Compared with conventional heat pipes, the evaporation and condensation sections, as well as the liquid and vapor flow lines of LHPs, are separated, and the wick medium only located in the evaporator of LHPs. Thus, LHPs exhibit high flexibility and long-distance heat transport capability against the gravity field [138,142,143]. Singh et al. [140] developed a miniature LHP installed inside the ECU of a vehicle with an evaporator attached to a semiconductor chip via a copper adapter and captive hardware and air-cooled condenser mounted with two centrifugal fans. Test results indicated that the miniature design of the LHP, with a 10 mm thick evaporator, was capable of transporting 70 W heat load up to a distance of 250 mm, while keeping the source temperature below the 100 °C limit. Meanwhile, two prototypes of LHPs with heat transfer distances of 250 and 1000 mm were able to achieve the maximum heat capacity of more than 500 W for adverse tilts in gravity.

To validate the LHP application for aircraft, the Europe Union recently launched a project named “HTCS” for efficient cooling of MEA [144]. By integrating passive cooling devices in the TMS, the maximal temperature of the equipment was expected to be significantly reduced. Advanced Cooling Technologies Inc. recently developed a series of passive thermal management devices for avionics cooling [15]. For example, to realize the internal temperature gradient reduction and improve heat sink availability, they developed a TMS for avionics cooling under high-temperature environments by using LHP and heat pipe assemblies, as shown in Figure 15 [125]. With the engine idling on the ground or flying at a low speed in the air, the cooling capacity of the fuel is generally low. In contrast, the air sinks show good performance in these scenarios. Therefore, a dual condenser scheme was developed to make full use of the limited heat sinks in the aircraft. This LHP with dual condensers could automatically identify the potential sinks to provide continuous heat rejection within the whole operating cycle. For example, one condenser interacts with the air sink, while the other is cooled by fuel or polyalphaolefin. Activating an alternative condensing section depends on the ambient temperatures of devices. During the operation, the LHP with multiple condensers will passively select the appropriate heat sink. Similarly, Vieira et al. [137] developed a two-phase loop thermosyphon by integrating one evaporator

with two condensers. It was designed to use the low temperatures of aircraft fuselage at high altitudes to facilitate passive avionics cooling. Accorinti et al. [132,145,146] proposed a new capillary pumped loop cooling system for power electronics on board hybrid propulsion aircraft. One or several parallel evaporators could be integrated in the primary loop. Experimental and numerical analysis indicated that the operating temperature of the power electronics was kept below the maximal junction temperature at a heat flux up to 242 W/cm^2. Moreover, the LHPs are also applied for anti-icing applications in aircraft, and considerable studies have been conducted to verify the anti-icing capacity and feasibility of the LHP ice protection system [147].

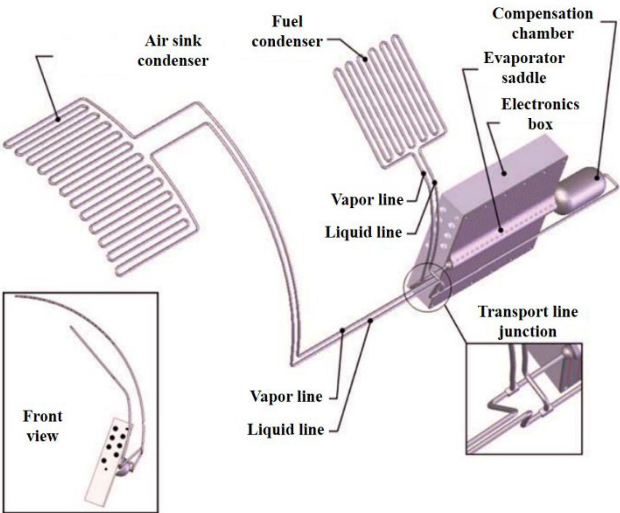

Figure 15. Schematic of the dual-condenser LHP [125].

3.1.4. Heat-Pipe-Based Hybrid Cooling Scheme

Despite that the TMS adopting an individual technique can provide a competing cooling capacity, a better comprehensive performance can be achieved via the combination and integration of several different thermal management techniques. For example, Cai et al. [129] combined the LHP and PHP to achieve long-distance and reliable heat transfer inside the avionics cooling systems. A 2-meter-long LHP using water as a coolant was developed to transport heat from the avionics chassis wall to the remote heat sink. Within the avionics chassis, the PHP was sandwiched with two PCBs via solder bonding to enhance the lateral heat transfer from electronics to the chassis wall. Figure 16 shows a schematic of the hybrid TMS and the LHP evaporator. Heat was transferred to the LHP evaporator via the tightly fitted clamps and chassis wall. Experimental demonstration of the LHP and PHP combo system indicated that the heat source temperature was maintained below 150 °C at a maximum input power of 400 W. Tecchio et al. [130] experimentally evaluated the thermal performance of a passive cooling system for heat sources on board aircraft. A heat exchanger system was designed to remove heat from the avionics via heat pipes serving as intermediate heat transfer elements. The heat exchanger system consisted of a shared evaporator and two parallel condensers. One condenser was oriented at the fuselage, while the other one was thermally coupled with the air-conditioning system. It was found that the average temperature of the avionics could be maintained below 70 °C. Zilio et al. [131] developed a hybrid active–passive cooling system by combining an LHP with an air-cooled mini vapor cycle system for helicopter avionics thermal management. The LHP was used for eliminating the heat spots on the avionics at the blade level, while the mini vapor cycle system was designed for the overall heat rejection. Experimental assessment demonstrated that the system performance was strongly affected by the ambient temperature because it controlled the condensing temperature. As a result, the device temperature sharply increased as the air ambient temperature increased. The maximum

allowable temperature of 120 °C was not exceeded at a heat load of 40 W and an ambient temperature up to 55 °C.

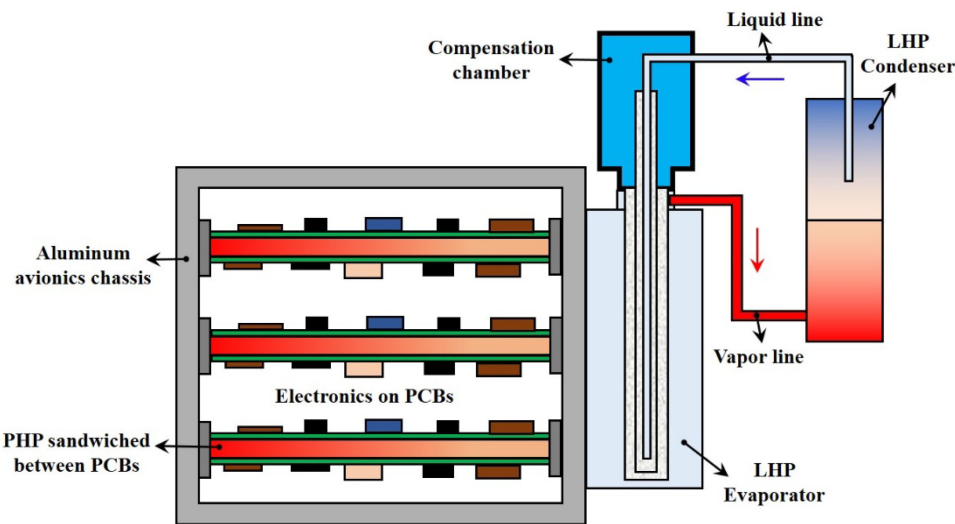

Figure 16. Schematic of the hybrid passive cooling system [129].

3.2. Phase Change Materials (PCMs)

During the practical operation of electric devices on board vehicles and aircraft, the power load and the corresponding heat load are usually subject to periodic or nonperiodic fluctuations. Moreover, the sharp power peaks are usually greater than the average power within one duty cycle. Accordingly, the thermal profiles of these electronics are often characterized by fluctuations and sharp peaks. In this regard, the transient thermal analysis is crucial to avoiding the overdesign of TMS in which the peak and valley thermal capacities fluctuate with varying magnitudes. In this scenario, PCMs do present particular advantages to cope with such problems [148,149].

Since the heat generation of the electronics is not constant, PCMs are usually adopted as thermal buffering in the TMS by temporarily storing the heat released by the electronics [10]. Tang et al. [150] embedded a PCM within the chip of the GaN transistor to serve as a microscale heat storage device, as shown in Figure 17. In this way, the heat capacity of the material could be effectively increased by taking advantage of the latent heat of the PCM. A 2-D transient thermal model was developed to predict the spatiotemporal temperature profile of the GaN transistor and characterize the PCM melting behavior and the dynamic evolution of hot spots within the device. Results demonstrated that the integration of the PCM in GaN transistors could significantly reduce the hot spot temperature at a given heat input. For example, the peak temperature of the hot spot could be reduced by 21–22 °C at a heat flux of 5×10^5 W/cm^2. Orr et al. [151] presented a transient thermal analysis of an IGBT inverter using a thermal resistance–capacitor network. A sample heat sink integrated with a PCM was modelled and then experimentally tested to validate the numerical model. The PCM integrated with the heat sink was identified as a potential method to reduce the peak of a chip temperature. According to the comparison of different PCM locations, it was suggested that the PCM should be located as close to the heat source as possible to enable a faster thermal time response [152].

When incorporating PCMs in either the electronic assemblies or the TMS, the selection of an optimal PCM should be carefully considered. In general, the selection of PCMs depends on the suitable melting point and the average heat source temperature at saturation. Besides, the features of high latent heat, high thermal conductivity, low volume change ratio, low density, and low cost are also desired. However, a tradeoff among these factors should be made in practical applications. For example, metallic PCMs with high thermal conductivity present a fast thermal response, but the large weight, cost, and integration complexity limit their viable applications. On the contrary, the commonly used organic

PCMs have high latent heat and low cost characteristics, but present poor heat transfer performance due to the low conductivity [152,153]. Usually, minimizing the weight and volume of the aircraft TMS plays an important role in reducing the total cost. Hence, many lightweight PCMs, such as paraffins, are widely adopted in practical applications. Pal et al. [154] investigated the transient thermal control performance of a PCM device, which was filled with an organic PCM, n-triacontane, in a honeycomb plate for cooling an avionics module. The numerical results over a single-cell model indicated that the effect of natural convection on the melting process was negligible for the power levels considered. Remotely located and intermittently or periodically operated electronics on aircraft always present a particularly difficult challenge when providing cooling for them. To cope with this challenge, Fossett et al. [155] developed a TMS with microencapsulated PCMs for such applications. The PCMs (MicroPCM^{TM} 143) were encapsulated into micro-sized particles with the diameter ranging from 30 to 50 microns. Results showed that a large weight reduction could be obtained by using the microencapsulated PCM technology rather than a solid aluminum plate for a passive heat sink. In addition, PCMs can also be adopted for a passive backup cooling scheme in case of failure in an active cooling scheme. In this way, a catastrophic failure in electronics functions could be avoided by allowing the safe return to the ground.

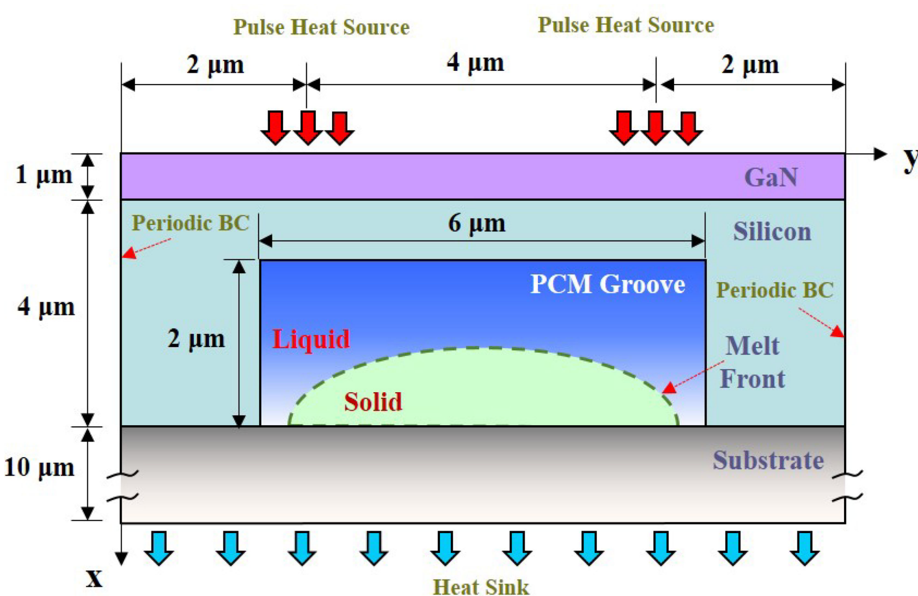

Figure 17. Schematic of the thermal model of a transistor unit with a microscale PCM groove [150].

On the other hand, the low thermal conductivity of PCMs can decrease the heat transfer efficiency of TMS, and the heat transfer enhancement techniques play an important role when using PCMs. For example, Nafis et al. [156] investigated the thermal performance of a passive heat sink filled with PCMs via numerical simulations. It was shown that a more uniform temperature distribution with lower peaks and smaller temperature fluctuations could be obtained by using a PCM, such as xylitol. As a result, the lifetime of the automotive electronic devices could be significantly improved. Meanwhile, the PCM (particularly organic) also increased the thermal resistance from the die to the ambient (or coolant) due to the low conductivity of PCMs. Thus, it was suggested to adopt the PCM with thin PCM layers. Over the last decades, various methods have been extensively studied to improve the heat transfer performance when applying PCMs in a TMS. Generally, the heat transfer enhancement can be achieved through either geometric optimization or thermal conductivity improvement [157–160]. Saha et al. [161] evaluated the performance and effectiveness of a PCM thermal storage unit of eicosane with aluminum pin fins at different volumetric percentages of a thermal conductivity enhancer (0%, 2%, 8%, 18%, and 27%). It was found that the case with 8% volumetric percentage of metal fins performed the

best. Moreover, the heat transfer enhancement techniques can also depress the nonuniform temperature profile in the PCM-based heat sinks. Actually, one major reason for the mechanical failure of electronics is the thermal stress induced by the nonuniform temperature distribution. Recently, Wu et al. [162] designed an orthotropic plate at the bottom of the heat sink to refine the temperature uniformity in the heat sink, especially in the PCM region. It was found that the temperature uniformity in the PCM regions could be significantly improved by up to four times, and the temperature range in the heat sink region could be narrowed down.

4. Environmental Influences on the TMS

As mentioned in Section 1, in the harsh automotive environment, the electronics and the corresponding TMS may undergo various types of mechanical load, such as the vibration due to road bumps [14,124]. Meanwhile, the fighter aircraft may frequently perform deceleration, acceleration, and maneuvering flight, thus introducing additional mechanical loads to the onboard equipment. The vibration amplitudes can reach about 10 g within a wide frequency band in commercial automobile engines and transmissions, while the shocks may even reach 30–1200 g in military combat vehicles [14]. As a matter of fact, the vibrations and shocks can severely impact the reliability of the electric devices and the corresponding TMS. For example, the vibration-induced effects can accelerate the fatigue failure and performance deterioration of the electronics and cooling components. In addition to the vibrations and shocks, the acceleration and gravity effects encountered in the automobiles and aircraft may pose apparent influences on the thermal fluidic behaviors inside the cooling system. Generally, most studies related to the electronics TMS on board automobiles and aircraft considered the normal operating mode. However, investigations focusing on the effects of a harsh environment, including vibrations, shocks, acceleration, and loss/hypergravity, on the TMS of automobiles and aircraft are severely insufficient, which will be discussed in this section.

4.1. Vibrations and Shock

4.1.1. Effects of Vibrations and Shock on Active TMS

Generally, as far as the heat exchangers within the active TMS are concerned, the heat transfer performance can be improved when they are exposed to the vibration environment. Li et al. [163] applied a vibration-enhanced heat transfer technology to improve the heat dissipation efficiency of a fin-tube radiator. The effects of vibrations on the thermal hydraulic performance of the radiator were analyzed via numerical simulation and wind tunnel tests. Results demonstrated that the vibrations could not only increase the heat transfer coefficient of the radiator but also apparently increase the pressure drop. The average heat flux density on the fin surface significantly increased as the vibration intensity increased. Similarly, the numerical model of a rectangular heat exchanger unit channel under vibration conditions was established by Fu et al. [164] to investigate the effects of vibrations on the heat transfer performance. The coupling effect of vibration frequency, amplitude, and inlet velocity on heat transfer characteristics was investigated. Results indicated that the vibration amplitude presented much more apparent effects in enhancing heat transfer in comparison with the vibration frequency. However, when the amplitude was larger than 4 mm, the pressure drop would rapidly increase. For the practical vehicle operation, the heat transfer performance could be effectively improved at an amplitude of 2 mm and a frequency of 25 Hz.

Apart from using vibration to enhance the thermal performance, vibration and shock isolation techniques are usually adopted to protect the sensitive components of the active cooling system. Hosseinloo et al. [165] performed a comprehensive set of random vibration and shock tests over a novel double-chamber jet impingement cooling system. Note that isolators with optimum performance were selected to reinforce the chassis containing the cooling chamber against shock and random vibrations in this system. The cooling performance was evaluated under both isolated and hard-mounted conditions with the

overall input vibration level ranging from 4 to 31 g. Results demonstrated that the cooling performance was not significantly affected by the vibrations and shocks, and the isolation system could protect the cooling system well.

Moreover, the vibrations can also weaken the heat transfer performance in some cases. Wang et al. [166] numerically investigated the effects of vibration on the local heat transfer characteristic process of the spray cooling process. A two-phase flow model was established by using the VOF method. The impacting of droplets on the film with a vapor bubble growing was selected as the local characteristic process. Results indicated that vibrations could apparently weaken the heat transfer with higher frequency and amplitude. In addition, when little liquid dropped on the surface, the phenomenon of liquid spatter induced by the vibration could be observed.

4.1.2. Effects of Vibrations and Shocks on Heat Pipes

In general, the liquid–vapor meniscus in the evaporator wick could be broken by the resonant vibrations, thus deteriorating the performance of the capillary devices. Moreover, the vapor/liquid distribution in the pipe lines of the loop can also be disturbed by mechanical shocks. As a result, both the startup behaviors and the long-term operation characteristics could be apparently affected. To tackle this issue, Tang et al. [14] developed a novel vibration/shock-tolerant capillary two-phase loop (CTPL) device as cooling alternatives for future military vehicles. Different from the traditional LHPs and CPLs, a graded wick structure was specially designed for the capillary evaporator. To counter the disturbances induced by the vibrations and shocks, the fine pores were used to provide stronger capillary action. Besides, a secondary wick with high permeability was applied to quickly replenish the liquid in the primary wick to avoid dryout caused by shocks. By using this graded wick designs, the impact of vibrations and shocks could be mitigated, and a high heat flux removal capability could be achieved. Then, a prototype of the CTPL was developed, and its performance was evaluated using variable heat inputs under multiple shocks up to 6.6 g. Results indicated that the CTPL exhibited good thermal behavior during both startup and normal operations.

Note that the influence mechanism of the vibrations on the performance of heat pipes is inconclusive. Hsu et al. [167] investigated the effects of vibrations and shocks on a sintered heat pipe by using the vibration and shock machine. Experiments were performed at a basic shock of 40 g and a random vibration frequency ranging from 5 to 100 Hz. Results demonstrated that the vibrations could slightly increase the thermal resistance, while the temperature and thermal resistance were almost not affected by the instant impact in shock testing. Alaei et al. [168] developed a vertical wickless heat pipe, and its thermal performance was evaluated under low-frequency vibration conditions. Results indicated that the thermal resistance for all tests was decreased as the low-frequency vibration increased from 0 to 30 Hz. Besides, the heat transfer coefficients of both condensation and boiling increased with the increase in vibration frequency. To understand the effect of vibration frequency on the thermal performance of a miniature LHP, Kumar et al. [169] performed an experimental study using an ammonia charged miniature LHP under both the transverse and longitudinal harmonic vibration conditions with a frequency of 15–45 Hz. Results showed that the thermal performance of the miniature LHP was not obviously affected by the acceleration rate and frequency of imposed transverse vibrations. In contrast, for the longitudinal vibration conditions, the performance was apparently enhanced due to increased acceleration. Essentially, the performance of the miniature LHP was mainly determined by the heat leak, which was strongly guided by fluid distribution. Singh et al. [140] tested an LHP subjected to random vibrations with a frequency range of 100–2000 Hz. It was found that the performance was slightly improved during the vibration tests. The authors attributed this improvement to the enhanced liquid distribution and agitation inside the evaporator core due to vibrations.

4.1.3. Effects of Vibrations on PCMs

The mechanical vibrations can apparently affect the melting processes of the PCMs, thus affecting the thermal performance of the passive TMS using PCMs [170]. In general, research focusing on the effects of vibrations on PCMs used for thermal management of electronics on board automobiles is extremely limited. Meanwhile, investigations on the effects of vibrations on PCMs used in the battery TMS of EVs can be used for reference. For example, Joshy et al. [171] investigated the effects of vibrations on the thermal field behavior of PCM inside a passive battery TMS. Experiments were performed at the vibration frequency ranging from 20 to 30 Hz and the amplitude ranging from 30 to 50 mm, which were typically observed in HEVs on the road during normal operation. It was found that the temperature at the battery surface increased with increasing frequency and vibration amplitude. For the solid phase of PCM, the effects of frequency and amplitude change on the surface temperature were not significant. In contrast, the vibration frequency and amplitude could apparently affect the battery surface temperature because of the natural convection circulation of liquid PCM. Besides, it was concluded that the PCM melting process could be enhanced by vibrations, thus shortening the effective operating time of the passive TMS in a practical driving test. Recently, Wu et al. [172] numerically studied the effects of vibration frequency and orientation of the vibration axis on the melting processes of PCMs. It was found that the melting processes could be critically accelerated by the enhanced mixing of molten PCMs under low-frequency vibration conditions. However, the time-averaged heat transfer rate was lower than its counterpart without vibrations. In contrast, an obviously faster charging speed was observed under higher vibration frequency conditions, but the acceleration effect became weak against the increasing of vibration frequency. Moreover, the melting process was apparently affected by the orientation of the vibration axis. When the vibration axis was parallel to the gravity direction, the charging speed and thermal response rate were fastest. Zhang et al. [173] experimentally investigated the effects of mechanical vibration on the battery TMS using composite PCMs, where high thermal conductivity elements, such as carbon nanoparticles and graphene, were added. Experiments were performed at a vibration amplitude of 2–4 mm and a frequency of 10–30 Hz. The combined effects of vibration frequency, vibration amplitude, and composition of the composite PCMs were analyzed. Results demonstrated that the small vibration amplitude showed great benefit to enhancing the heat transfer of composite PCMs and lowering the battery's operating temperature. Meanwhile, the heat transfer efficiency of the TMS could be apparently improved by the acceleration of the dispersion and collision of the high thermal conductivity particles in composite PCMs. However, the very high or very low vibration frequency was not conducive to enhancing heat transfer, and 20 Hz was found to be the optimal frequency within the considered range.

4.2. Acceleration and Gravity

4.2.1. Effects of Gravity on Active TMS

The alterations in the gravity brought by the abrupt maneuvering of the aircraft will introduce some concerns in the application of the active TMS. For example, the droplet heat transfer and flow pattern of the spray cooling system are significantly affected by gravity. The influence mechanism of gravity on the fluid flow behavior and the cycling and management of the two-phase flows is still not clear, thus making it difficult to control the heat transfer process effectively and accurately [41]. Currently, studies on the gravity effects in the spray cooling system are mainly related to the development of a TMS for spacecraft operating under a weightless environment. The open literature reporting the effects of hypergravity and gravity orientation on the performance of such active TMSs is scarce. Zhao et al. [174] investigated the surface orientation effects on the heat transfer performance of a spray cooling system. It was observed that the CHF was obviously dependent on the surface orientation in medium-spray volumetric fluxes. The CHF of the case with a vertical surface was higher than that of the cases with upward and downward surfaces. However, the orientation dependency of the CHF was reduced with the increase in inlet pressure.

Besides, the surface liquid film flow and temperature distribution were almost not affected by the surface orientation. The interaction between vapor and spray (or the surface wall) was verified to be the main mechanism affecting the orientation dependence by intermittent spray cooling. To quantitatively evaluate the orientation effects, a semiempirical macrolayer model for the critical heat flux was proposed.

4.2.2. Effects of Acceleration on Heat Pipes

The acceleration or deceleration, which are always encountered during the driving process of vehicles and the takeoff and landing stages of aircraft, shows adverse effects on the performance of the heat pipes. For example, when the capillary action is not sufficient to overcome the unfavorable acceleration, the liquid in the condenser cannot successfully return to the LHP condensation chamber, thus causing the wick to dry out [147]. Ku et al. [175,176] experimentally investigated the effects of acceleration on the performance of LHPs. A miniature LHP was mounted on a rotary table and subjected to variable acceleration forces by rotating the table at different angular speeds. The centrifugal acceleration was acting in a direction parallel to the axis of the evaporator condensation chamber. The centrifugal accelerations ranged from 1.2 to 4.8 g. Results indicated that the superheat seemed to be independent of either the heat load or the acceleration force. Furthermore, the temperature overshoot appeared to be dependent more on the thermal load than on the accelerating force. The fluid distribution in the evaporator, condenser, and condensation chamber could be apparently affected by the changes in the accelerating force, thus leading to the temperature oscillation. Fleming et al. [177] experimentally investigated the behavior of a titanium–water LHP under standard and elevated acceleration fields. They found that dryout was dependent on both heat load at the evaporator and radial acceleration. Besides, the ability of the LHP to reprime after the dryout induced by the acceleration was dependent on the evaporator temperature. For high thermal load conditions, when the superheat of the evaporator wall slightly increased with the radial acceleration, there was no significant relationship between the evaporative heat transfer coefficient and the radial acceleration. Xie et al. [178,179] investigated the operating characteristics of a novel dual condensation chamber LHP under terrestrial gravity and elevated acceleration conditions. In order to provide the acceleration up to 7 g with different acceleration directions, a centrifuge with a 2 m long arm was adopted in the experimental facility. Some specific operating behaviors of the LHP were observed because of the vapor–liquid redistribution induced by the acceleration force. Besides, the operation of the LHP was found to be sensitive to the acceleration direction only at small heat load conditions. The acceleration magnitude could alter the operating mode. The transition of the operation mode was dependent on the acceleration directions, magnitudes, and heat loads. In addition, temperature fluctuation and reverse flow phenomena were observed under elevated acceleration fields. The temperature fluctuations could be suppressed by the acceleration, while they could provoke reverse flow. Recently, they further investigated the transient operating performance of the LHP incorporating with a TEC under acceleration conditions [180]. Results indicated that not only the operating performance could be improved by using the TEC, but also the operating temperature at a small heat load and acceleration magnitude could be reduced. In contrast, when the acceleration exceeds 3 g at a large heat load, the effects of TEC assist on the operation was negligible.

4.2.3. Effects of Gravity on Heat Pipes

Nagano et al. [181] investigated the effects of gravity on the heat transfer characteristics in a miniature LHP with multiple evaporators and multiple condensers. Experimental tests were performed in three different orientations, namely, horizontal, 45° tilt, and vertical. Results indicated that the LHP natural operating temperature was apparently affected by the gravity when the condensation temperature was not actively controlled. An increasing adverse elevation led to a higher natural operating temperature. Besides, the heat transport capability decreased with an increasing adverse elevation due to the additional gravity

head. In the vertical case, the secondary wick was unable to pump the liquid from the condensation chamber to the evaporator against the gravity. The operating characteristics were strongly dependent on the initial liquid distribution between the evaporator and the condensation chamber. However, the initial liquid distribution was not known before the experiments, thus leading to the LHP performance becoming unpredictable. Nakamura et al. [142] evaluated the gravity effects on the heat transfer characteristics of a 10 m long-distance LHP. Results indicated that the antigravity effect of the LHP degraded the heat transfer efficiency due to the increase in heat leak from the evaporator to the condensation chamber. Moreover, developing novel wicks is an effective approach to improve the antigravity capability of heat pipes. By taking both the mechanical property and the thermal performance into consideration, a vapor chamber with novel compound columns was developed by Liu et al. [182]. The columns consisted of many solid copper bars and porous functional structures sintered onto the cylinder surface of the pillars. The thermal behavior of vapor chambers was evaluated under different inclination tilts to verify the superiority of the compound columns. Results demonstrated that the capillary limit and the recycle of the working fluid were improved by the cladding layers of the columns in the antigravity position, thus broadening the adaptability of the vapor chamber.

4.2.4. Effects of Gravity on PCMs

The exposure of PCM to hypergravity during the maneuvering flight of aircraft may greatly affect its thermal performance, as depicted in Figure 18a. To reveal the melting heat transfer characteristics under hypergravity conditions, Xu et al. [183] experimentally studied the melting process of n-docosane ($C_{22}H_{46}$) under different hypergravities. Results showed that when the heat flux was constant, an increase in hypergravity could accelerate melting and lower the heating wall temperature due to the enhanced heat convection inside the liquid PCM. Compared with the cases under normal gravity, the time required for complete melting and the corresponding heating wall temperature under hypergravity conditions were reduced by 20.6% and 21.0%, respectively. Besides, increasing heat flux under constant hypergravity could accelerate the melting rate and increase the heating wall temperature. However, as the heat flux increased, the effect was suppressed by the hypergravity-enhanced heat convection. Then, they further investigated the melting behaviors of an n-docosane based a pin fin heat sink and an empty heat sink without pin fins under a hypergravity of 0–6 g [184]. Results demonstrated that the melting process was significantly affected under hypergravity conditions, but the effects were weakened by increasing hypergravity. The heating wall temperature under hypergravity conditions was lower than that under a normal condition. For an empty heat sink, the complete melting time decreased with increasing hypergravity, while it increased for the pin fin heat sink. It was indicated that the heat transfer enhancement by pin fins was counteracted by their inhibition of heat convection of liquid PCM under hypergravity. For cases with large heat flux, the complete melting time was shortened by adding pin fins at any hypergravity. In contrast, this time was extended for a small heat flux case under hypergravity. Moreover, the increasing hypergravity might lead to the increase in the dip angle of the liquid level, as well as the width of the unsubmerged area on the heating wall, which might lead to overheating damage. Tang et al. [185] investigated the acceleration effect on paraffin melting in a finned copper foam energy storage unit filling with n-eicosane. Experiments were performed at a heat flux of 0.4–0.55 W/cm^2 and centrifugal acceleration magnitudes ranging from 0 to 13 g with three different acceleration directions. It was found that the thermal performance was dependent on the placement method of the heat flux and acceleration directions, as shown in Figure 18b. For the cases of vertical and opposite directions, the thermal performance was improved, while it was restrained for the case of the same direction. Compared with the case of vertical direction, the average melting time for the cases of opposite and similar directions increased by 15.19% and 37.10%, respectively. Moreover, the melting time decreased as the acceleration magnitude along the vertical and the same directions increased. The temperature difference of the phase change energy

storage unit decreased with the increasing acceleration magnitude along vertical direction, but increased along the opposite or same direction.

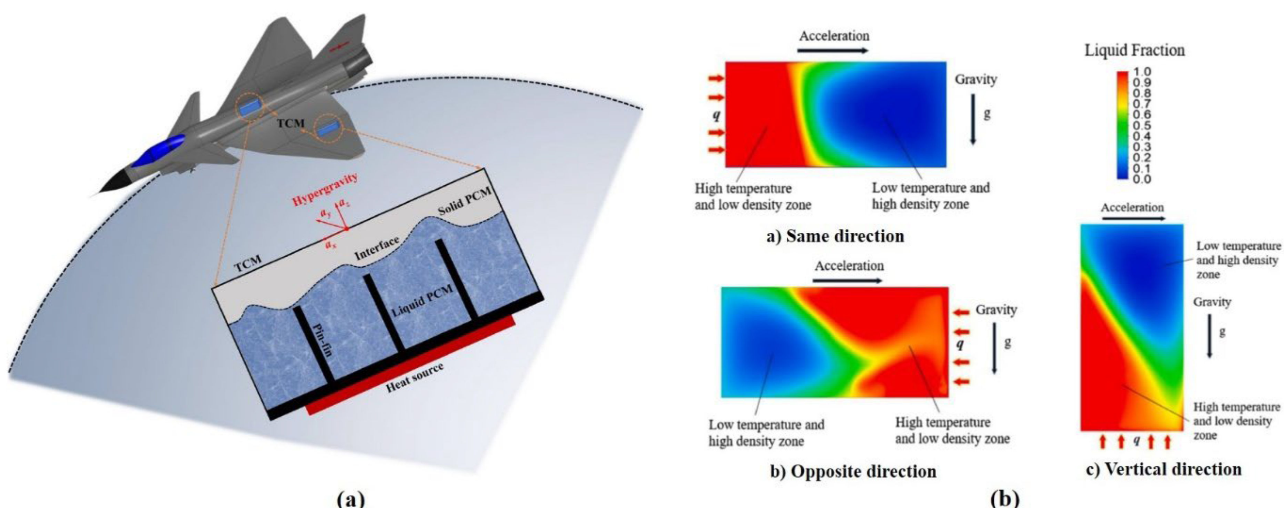

Figure 18. Schematic of (**a**) the PCM device on board aircraft under hypergravity condition and (**b**) PCM melting process in different acceleration directions [183,185].

5. Conclusions and Remarks

The present paper addressed the thermal challenges of electronics with high heat flux on board automobiles and aircraft in detail. In addition to developing WBG semiconductors with satisfactory electric and thermal performance, applying proper thermal management solutions should be a much more cost-effective way at present. Moreover, the thermal management in automobiles and aircraft applications will be much more crucial in the coming future due to the increasing power and minimizing size of applied electronics. This paper provides the structural characteristics, thermal performance, and development tendency in active and passive thermal management technologies. The advantages and disadvantages of various thermal management technologies are summarized, as shown in Table 8. Moreover, the environmental influences, including vibration, shock, and acceleration, on the thermal performance and reliability of the TMS are also emphasized and discussed in detail. Based on the above discussions, some major conclusion can be drawn as follows:

Table 8. Comparison of various thermal management technologies for electronics on board automobiles and aircraft.

Thermal Management Technology	Advantages		Disadvantages
Forced air cooling	Compact, simple layout, and low cost		Low heat transfer efficiency
Indirect contact cold plate cooling	Single-phase	Higher heat transfer efficiency in comparison with forced air cooling, high controllability, and high scalability	Poor temperature uniformity, low stability for temperature control, and the heat dissipation capacity is greatly dependent on the flow rate
	Two-phase	Much higher heat transfer efficiency, lower flow rates, more uniform surface temperature, and lower pumping power	Complicated loop layout, flow instability, and low technology readiness level
Direct contact baseplate cooling	Higher heat transfer performance, more compact size, and lighter weight (compared with the indirect contact cold plate cooling)		Lower scalability and relatively poorer temperature uniformity (compared with the indirect contact cold plates cooling)
Jet impingement and spray cooling	Much higher heat dissipation capability		Much higher pressure loss and relatively lower controllability
Heat pipes	Excellent heat transfer efficiency and temperature uniformity, no power consumption, longer operational life, high layout flexibility, and low maintenance requirements		Limited heat dissipation capacity
PCMs	High reliability, high scalability, no power consumption, competitive for thermal load with varying magnitudes		Effective operating time is strongly dependent on the mass of PCMs

(1) Generally, active thermal management solutions via indirect contact cold plate and direct contact baseplate cooling are the most commonly adopted for electronics on board automobiles and aircraft. Although the jet impingement and spraying cooling can provide promising alternatives in these applications, they are not practically applied for electronics cooling in marketed automobiles and aircraft up to now. In this regard, more in-depth validation studies need to be conducted under such a harsh environment. In addition, despite that the forced air-cooling scheme is seldom implemented for traditional Si-based power electronics due to its lower heat transfer efficiency, it remains to be an attractive option for the next-generation WBG power electronics because of its advantages in improving the compactness and reducing the complexity and cost via the elimination of an additional cooling loop and many bulky components.

(2) The application of passive heat transfer devices, including heat pipes and PCMs, has been widely implemented. Various types of heat pipes are integrated in practical TMS and serve as a passive heat transfer component and/or a heat spreader with uniform cooling, thus greatly reducing the thermal resistance and improving the temperature uniformity of the electronic modules. Particularly, LHPs are much more attractive for heat sources remotely located to the heat sinks. Due to the fluctuated thermal profiles of the onboard electronics with sharp peaks, PCMs present great advantages in short-term overheat protection and thermal buffering in the TMS by temporarily storing the heat released by the electronics. As a result, the cooling capacity can be determined based on the average power rather than the peak power of the cycle, thereby avoiding the overdesign and reducing the mass and cost of the TMS. Note that the transient thermal analysis is required to determine the suitability of a heat sink and ensure the max peak temperature within the safe operating ranges.

(3) Considering the distributed configuration and specific requirements for different heat sources, the application of a hybrid TMS is much more promising, which incorporates several thermal management techniques and makes full use of them. Usually, the combination of two or more cooling techniques in the TMS exhibits a much better comprehensive performance, and this may be an important development tendency for the TMS design in the future. In this regard, the highly efficient incorporation of various techniques in the hybrid system draws more attention.

(4) Since the designs on electrical, mechanical, and thermal considerations are tightly interconnected, the changes in any one design will have apparent consequences on the others. Hence, the above three systems for power electronics should be considered simultaneously. It is extremely necessary to develop comprehensive and multidisciplinary optimization strategies, featuring easy iteration for the overall performance improvement.

(5) Due to the multiple constraints posed by the operating environments, antivibration, antishock, and gravity insensitivity of the TMS design are of great importance, especially for cases where a phase transition of the working medium occurs, for example, the active two-phase mechanical pumped fluid loop, heat pipes, and PCMs. Before the practical application of TMS in engineering operation, the experimental testing under simulated harsh environments is essential for ensuring the long-term reliability due to the complex dynamic operating characteristics.

Currently, most studies investigate the TMS for electronics on board automobiles and aircraft only in a normal operating mode. Studies on the effects of harsh environmental factors, including vibrations, shocks, acceleration, and loss/hypergravity, are severely insufficient. Thus, further investigations need to be performed to gain systematic and in-depth knowledge of the thermal fluidic behaviors of the working medium inside the TMS under harsh environments.

Author Contributions: Writing-original draft preparation, Y.-G.L.; writing—review and editing, visualization, supervision, G.-P.Z., Q.-W.W. and W.-X.C. All authors have read and agreed to the published version of the manuscript.

Funding: This research was funded by the National Natural Science Foundation of China (Grant No. 52206113) and the Youth Innovation Promotion Association, CAS (Grant No. 2022410).

Conflicts of Interest: The authors declare no conflict of interest.

Nomenclature

AEV	All-electric vehicle
CHF	critical heat flux
CTPL	capillary two-phase loop
DBC	directed bonding copper
ECU	engine control unit
EV	electric vehicle
HEV	hybrid electric vehicle
LHP	loop heat pipe
MEA	more electric aircraft
MOSFET	metal–oxide–semiconductor field-effect transistor
PCM	phase change material
PCU	power control unit
PHP	pulsating heat pipe
TCU	transmission control unit
TEC	thermoelectric cooler
TIM	thermal interface material
TMS	thermal management system
ICEV	internal combustion engine vehicle
IGBT	insulated gate bipolar translators
VOF	volume of fluid
WBG	wide bandgap

References

1. Diaz, M.N. *Electric Vehicles: A Primer on Technology and Selected Policy Issues*; R46231; Congressional Research Service: Washington, DC, USA, 2020.
2. Huque, M.A.; Islam, S.K.; Blalock, B.J.; Su, C.; Vijayaraghavan, R.; Tolbert, L.M. Silicon-on-Insulator Based High-Temperature Electronics for Automotive Applications. In Proceedings of the 2008 IEEE International Symposium on Industrial Electronics, Cambridge, UK, 30 June–2 July 2008.
3. Nakayama, W.; Suzuki, O.; Hara, Y. Thermal Management of Electronic and Electrical Devices in Automobile Environment. In Proceedings of the 2009 IEEE Vehicle Power and Propulsion Conference, Dearborn, MI, USA, 7–10 September 2009.
4. Johnson, R.W.; Evans, J.L.; Jacobsen, P.; Thompson, J.R.R.; Christopher, M. The Changing Automotive Environment: High-Temperature Electronics. *IEEE Trans. Electron. Packag. Manuf.* **2004**, *27*, 164–176. [CrossRef]
5. Langmaack, N.; Tareilus, G.; Henke, M. Modular Power Electronics for Electric Vehicles and Aviation Applications. In Proceedings of the 2019 IEEE 13th International Conference on Power Electronics and Drive Systems (PEDS), Toulouse, France, 9–12 July 2019.
6. Liu, X.; Wu, Z.; Yan, Y.; Kang, Y.; Chen, C. A Novel Double-Sided Cooling Inverter Leg for High Power Density EV Based on Customized SiC Power Module. In Proceedings of the 2020 IEEE Energy Conversion Congress and Exposition (ECCE), Detroit, MI, USA, 11–15 October 2020.
7. Lai, J.-S.; Yu, W.; Qian, H.; Sun, P.; Ralston, P.; Meehan, K. High Temperature Device Characterization for Hybrid Electric Vehicle Traction Inverters. In Proceedings of the 2009 Twenty-Fourth Annual IEEE Applied Power Electronics Conference and Exposition, Washington, DC, USA, 15–19 February 2009.
8. Passmore, B.S.; Lostetter, A.B. A review of SiC power module packaging technologies Attaches, interconnections, and advanced heat transfer. In Proceedings of the 2017 IEEE International Workshop on Integrated Power Packaging (IWIPP), Delft, The Netherlands, 5–7 April 2017.
9. Hassan, A.; Savaria, Y.; Sawan, M. Electronics and Packaging Intended for Emerging Harsh Environment Applications: A Review. *IEEE Trans. Very Large Scale Integr. VLSI Syst.* **2018**, *26*, 2085–2098. [CrossRef]
10. Jankowski, N.R.; McCluskey, F.P. A review of phase change materials for vehicle component thermal buffering. *Appl. Energy* **2014**, *113*, 1525–1561. [CrossRef]

11. Robles, J. A system level view of Avionics—Vetronics cooling options for harsh environment two-level maintenance systems. In Proceedings of the Twentieth Annual IEEE Semiconductor Thermal Measurement and Management Symposium, San Jose, CA, USA, 11 March 2004.
12. Korta, J.; Skruch, P.; Holon, K. Reliability of Automotive Multidomain Controllers: Advancements in electronics cooling technologies. *IEEE Veh. Technol. Mag.* **2021**, *16*, 86–94. [CrossRef]
13. Yang, D.; Liu, D.; Driel, W.D.v.; Scholten, H.; Goumans, L.; Faria, R. Advanced reliability study on high temperature automotive electronics. In Proceedings of the 2010 11th International Conference on Electronic Packaging Technology & High Density Packaging, Xi'an, China, 16–19 August 2010.
14. Tang, X.; Park, C. Vibration/Shock-Tolerant Capillary Two-Phase Loop Technology for Vehicle Thermal Control. In Proceedings of the 2008 ASME Summer Heat Transfer Conference, Jacksonville, FL, USA, 10–14 August 2008.
15. Ellis, M.; Montgomery, J. Passive Thermal Management for Avionics in High Temperature Environments. In Proceedings of the SAE 2014 Aerospace Systems and Technology Conference, Cincinnati, OH, USA, 23–25 September 2014.
16. Brewer, R.A. High temperature electronics for demanding aircraft applications. In Proceedings of the 2018 International Applied Computational Electromagnetics Society Symposium (ACES), Denver, CO, USA, 25–29 March 2018.
17. Mc Cluskey, P.; Saadon, Y.; Yao, Z.; Shah, J.; Kizito, J. Thermal Management Challenges in Turbo-Electric and Hybrid Electric Propulsion. In Proceedings of the 2018 International Energy Conversion Engineering Conference, Cincinnati, OH, USA, 9–11 July 2018.
18. Jafari, S.; Nikolaidis, T. Thermal Management Systems for Civil Aircraft Engines: Review, Challenges and Exploring the Future. *Appl. Sci.* **2018**, *8*, 2044. [CrossRef]
19. Wileman, A.J.; Aslam, S.; Perinpanayagam, S. A road map for reliable power electronics for more electric aircraft. *Prog. Aerosp. Sci.* **2021**, *127*, 100739. [CrossRef]
20. Mao, Y.F.; Li, Y.Z.; Wang, J.X.; Xiong, K.; Li, J.X. Cooling Ability/Capacity and Exergy Penalty Analysis of Each Heat Sink of Modern Supersonic Aircraft. *Entropy* **2019**, *21*, 223. [CrossRef]
21. Pal, D.; Severson, M. Liquid Cooled System for Aircraft Power Electronics Cooling. In Proceedings of the 2017 16th IEEE Intersociety Conference on Thermal and Thermomechanical Phenomena in Electronic Systems (ITherm), Orlando, FL, USA, 30 May–2 June 2017.
22. Ohadi, M.; Qi, J. Thermal Management of Harsh-Environment Electronics. In Proceedings of the Twentieth Annual IEEE Semiconductor Thermal Measurement and Management Symposium (SEMI-THERM), San Jose, CA, USA, 11 March 2004; pp. 231–240.
23. Garimella, S.V.; Fleischer, A.S.; Murthy, J.Y.; Keshavarzi, A.; Prasher, R.; Patel, C.; Bhavnani, S.H.; Venkatasubramanian, R.; Mahajan, R.; Joshi, Y.; et al. Thermal Challenges in Next-Generation Electronic Systems. *IEEE Trans. Compon. Packag. Technol.* **2008**, *31*, 801–815. [CrossRef]
24. Laloya, E.; Lucia, O.; Sarnago, H.; Burdio, J.M. Heat Management in Power Converters: From State of the Art to Future Ultrahigh Efficiency Systems. *IEEE Trans. Power Electron.* **2016**, *31*, 7896–7908. [CrossRef]
25. Iradukunda, A.-C.; Huitink, D.R.; Luo, F. A Review of Advanced Thermal Management Solutions and the Implications for Integration in High-Voltage Packages. *IEEE J. Emerg. Sel. Top. Power Electron.* **2020**, *8*, 256–271. [CrossRef]
26. Ghaisas, G.; Krishnan, S. A Critical Review and Perspective on Thermal Management of Power Electronics Modules for Inverters and Converters. *Trans. Indian Natl. Acad. Eng.* **2021**, *7*, 47–60. [CrossRef]
27. Mathew, J.; Krishnan, S. A Review on Transient Thermal Management of Electronic Devices. *J. Electron. Packag.* **2021**, *144*, 010801. [CrossRef]
28. Zuo, J.; Anderson, W.; Bonner, R. Advanced Thermal Management Technologies for High Power Automotive Equipment. In Proceedings of the National Defense Industrial Association Ground Vehicle Power and Energy Workshop, Troy, MI, USA, 18–19 November 2008.
29. Broughton, J.; Smet, V.; Tummala, R.R.; Joshi, Y.K. Review of Thermal Packaging Technologies for Automotive Power Electronics for Traction Purposes. *J. Electron. Packag.* **2018**, *140*, 040801. [CrossRef]
30. Lajunen, A.; Yang, Y.; Emadi, A. Recent Developments in Thermal Management of Electrified Powertrains. *IEEE Trans. Veh. Technol.* **2018**, *67*, 11486–11499. [CrossRef]
31. López, I.; Ibarra, E.; Matallana, A.; Andreu, J.; Kortabarria, I. Next generation electric drives for HEV/EV propulsion systems: Technology, trends and challenges. *Renew. Sustain. Energy Rev.* **2019**, *114*, 109336. [CrossRef]
32. Marshall, G.J.; Mahony, C.P.; Rhodes, M.J.; Daniewicz, S.R.; Tsolas, N.; Thompson, S.M. Thermal Management of Vehicle Cabins, External Surfaces, and Onboard Electronics: An Overview. *Engineering* **2019**, *5*, 954–969. [CrossRef]
33. Oh, S.K.; Lundh, J.S.; Shervin, S.; Chatterjee, B.; Lee, D.K.; Choi, S.; Kwak, J.S.; Ryou, J.-H. Thermal Management and Characterization of High-Power Wide-Bandgap Semiconductor Electronic and Photonic Devices in Automotive Applications. *J. Electron. Packag.* **2019**, *141*, 020801. [CrossRef]
34. Lu, M.-C. Comparative Study on a Power Module Architectures for Modularity and Scalability. *J. Electron. Packag.* **2020**, *142*, 040801. [CrossRef]
35. Yuan, R.; Fletcher, T.; Ahmedov, A.; Kalantzis, N.; Pezouvanis, A.; Dutta, N.; Watson, A.; Ebrahimi, K. Modelling and Co-simulation of hybrid vehicles: A thermal management perspective. *Appl. Therm. Eng.* **2020**, *180*, 115883. [CrossRef]

36. Abramushkina, E.; Zhaksylyk, A.; Geury, T.; El Baghdadi, M.; Hegazy, O. A Thorough Review of Cooling Concepts and Thermal Management Techniques for Automotive WBG Inverters: Topology, Technology and Integration Level. *Energies* **2021**, *14*, 4981. [CrossRef]
37. Jones-Jackson, S.; Rodriguez, R.; Emadi, A. Jet Impingement Cooling in Power Electronics for Electrified Automotive Transportation: Current Status and Future Trends. *IEEE Trans. Power Electron.* **2021**, *36*, 10420–10435. [CrossRef]
38. Previati, G.; Mastinu, G.; Gobbi, M. Thermal Management of Electrified Vehicles—A Review. *Energies* **2022**, *15*, 1326. [CrossRef]
39. Freeman, J.; Singh, R.; Osterkamp, P.; Green, M.; Gibson, A.; Schiltgen, B. Challenges and opportunities for electric aircraft thermal management. *Aircr. Eng. Aerosp. Technol.* **2014**, *86*, 519–524. [CrossRef]
40. Hendricks, T.J.; Tarau, C.; Dyson, R.W. Hybrid Electric Aircraft Thermal Management: Now, New Visions and Future Concepts and Formulation. In Proceedings of the 2021 20th IEEE Intersociety Conference on Thermal and Thermomechanical Phenomena in Electronic Systems (iTherm), San Diego, CA, USA, 1–4 June 2021; pp. 467–476.
41. Wang, J.; Li, Y.; Liu, X.; Shen, C.; Zhang, H.; Xiong, K. Recent active thermal management technologies for the development of energy-optimized aerospace vehicles in China. *Chin. J. Aeronaut.* **2021**, *34*, 1–27. [CrossRef]
42. Kelly, K.J.; Abraham, T.; Bennion, K.; Bharathan, D.; Narumanchi, S.; O'Keefe, M. Assessment of thermal control technologies for cooling electric vehicle power electronics. In Proceedings of the 23rd International Electric Vehicle Symposium (EVS-23), Anaheim, CA, USA, 2–5 December 2007.
43. Chinthavali, M.; Tawfik, J.A.; Arimilli, R.V. Design and analysis of a 55-kW air-cooled automotive traction drive inverter. In Proceedings of the 2011 IEEE Energy Conversion Congress and Exposition, Phoenix, AZ, USA, 17–22 September 2011.
44. Sato, S.; Matsui, K.; Zushi, Y.; Murakami, Y.; Tanimoto, S.; Sato, H.; Yamaguchi, H. Forced-Air-Cooled 10 kW Three-Phase SiC Inverter with Output Power Density of More than 20 kW/L. *Mater. Sci. Forum* **2011**, *679–680*, 738–741. [CrossRef]
45. Wrzecionko, B.; Bortis, D.; Kolar, J.W. A 120 °C Ambient Temperature Forced Air-Cooled Normally-off SiC JFET Automotive Inverter System. *IEEE Trans. Power Electron.* **2014**, *29*, 2345–2358. [CrossRef]
46. Liu, T.; Huang, Z.; Tan, Y.; Chen, C.; Zou, K.; Peng, H.; Kang, Y.; Luo, F. A high power density and high efficiency three phase inverter based on a hybrid 3D SiC packaging power module. In Proceedings of the 2018 IEEE Energy Conversion Congress and Exposition (ECCE), Portland, OR, USA, 23–27 September 2018.
47. Zeng, Z.; Zhang, X.; Blaabjerg, F.; Chen, H.; Sun, T. Stepwise Design Methodology and Heterogeneous Integration Routine of Air-Cooled SiC Inverter for Electric Vehicle. *IEEE Trans. Power Electron.* **2020**, *35*, 3973–3988. [CrossRef]
48. Li, Y.; Zhang, Y.; Yuan, X.; Zhang, L.; Song, Z.; Wu, M.; Ye, F.; Li, Z.; Li, Y.; Xu, Y.; et al. 500 kW Forced Air-Cooled Silicon Carbide (SiC) Three-Phase DC/AC Converter With a Power Density of 1.246 MW/m3 and Efficiency >98.5%. *IEEE Trans. Ind. Appl.* **2021**, *57*, 5013–5027. [CrossRef]
49. Chinthavali, M.; Christopher, J.F.; Arimilli, R.V. Feasibility study of a 55-kW air-cooled automotive inverter. In Proceedings of the 2012 Twenty-Seventh Annual IEEE Applied Power Electronics Conference and Exposition (APEC), Orlando, FL, USA, 5–9 February 2012.
50. Icoz, T.; Arik, M. Light Weight High Performance Thermal Management with Advanced Heat Sinks and Extended Surfaces. *IEEE Trans. Compon. Packag. Technol.* **2010**, *33*, 161–166. [CrossRef]
51. Buttay, C.; Rashid, J.; Johnson, C.M.; Ireland, P.; Udrea, F.; Amaratunga, G.; Malhan, R.K. High performance cooling system for automotive inverters. In Proceedings of the 2007 European Conference on Power Electronics and Applications, Aalborg, Denmark, 2–5 September 2007.
52. Qi, F.; Wang, M.; Xu, L. Investigation and Review of Challenges in a High-Temperature 30-kVA Three-Phase Inverter Using SiC MOSFETs. *IEEE Trans. Ind. Appl.* **2018**, *54*, 2483–2491. [CrossRef]
53. Zhang, C.; Srdic, S.; Lukic, S.; Kang, Y.; Choi, E.; Tafti, E. A SiC-Based 100 kW High-Power-Density (34 kW − L) Electric Vehicle Traction Inverter. In Proceedings of the 2018 IEEE Energy Conversion Congress and Exposition (ECCE), Portland, OR, USA, 23–27 September 2018.
54. Karimi, D.; Behi, H.; Jaguemont, J.; Baghdadi, M.E.; Mierlo, J.V.; Hegazy, O. Thermal Concept Design of MOSFET Power Modules in Inverter Subsystems for Electric Vehicles. In Proceedings of the 2019 9th International Conference on Power and Energy Systems (ICPES), Perth, WA, Australia, 10–12 December 2019.
55. Vetrovec, J. High-Performance Heat Sink for Interfacing Hybrid Electric Vehicles Inverters to Engine Coolant Loop. In Proceedings of the SAE 2011 World Congress & Exhibition, Detroit, MI, USA, 12–14 April 2021; SAE International: Warrendale, PA, USA, 2011.
56. Wang, P.; McCluskey, P. Evaluation of Two-Phase Cold Plate for Cooling Electric Vehicle Power Electronics. In Proceedings of the ASME 2011 International Mechanical Engineering Congress & Exposition, Denver, CO, USA, 11–17 November 2011.
57. Mancin, S.; Zilio, C.; Righetti, G.; Rossetto, L. Mini Vapor Cycle System for high density electronic cooling applications. *Int. J. Refrig.* **2013**, *36*, 1191–1202. [CrossRef]
58. Wang, P.; McCluskey, P.; Bar-Cohen, A. Hybrid Solid- and Liquid-Cooling Solution for Isothermalization of Insulated Gate Bipolar Transistor Power Electronic Devices. *IEEE Trans. Compon. Packag. Manuf. Technol.* **2013**, *3*, 601–611. [CrossRef]
59. Zhao, W.; France, D.M.; Yu, W.; Singh, D. Subcooled Boiling Heat Transfer for Cooling of Power Electronics in Hybrid Electric Vehicles. *J. Electron. Packag.* **2015**, *137*, 031013. [CrossRef]
60. Sakanova, A.; Tong, C.; Tseng, K.J.; Simanjorang, R.; Gupta, A.K. Weight Consideration of Liquid Metal Cooling Technology for Power Electronics Converter in Future Aircraft. In Proceedings of the 2016 IEEE 2nd Annual Southern Power Electronics Conference (SPEC), Auckland, New Zealand, 5–8 December 2016.

61. Sakanova, A.; Tong, C.F.; Nawawi, A.; Simanjorang, R.; Tseng, K.J.; Gupta, A.K. Investigation on weight consideration of liquid coolant system for power electronics converter in future aircraft. *Appl. Therm. Eng.* **2016**, *104*, 603–615. [CrossRef]
62. Aranzabal, I.; de Alegria, I.M.; Garate, J.I.; Andreu, J.; Delmonte, N. Two-phase liquid cooling for electric vehicle IGBT power module thermal management. In Proceedings of the 11th IEEE International Conference on Compatibility, Power Electronics and Power Engineering (CPE-POWERENG), Cadiz, Spain, 4–6 April 2017.
63. Olejniczak, K.; Flint, T.; Simco, D.; Storkov, S.; McGee, B.; Shaw, R.; Passmore, B.; George, K.; Curbow, A.; McNutt, T. A compact 110 kVA, 140°C ambient, 105°C liquid cooled, all-SiC inverter for electric vehicle traction drives. In Proceedings of the 2017 IEEE Applied Power Electronics Conference and Exposition (APEC), Tampa, FL, USA, 26–30 March 2017.
64. Gurpinar, E.; Wiles, R.; Ozpineci, B.; Raminosoa, T.; Zhou, F.; Liu, Y.; Dede, E.M. SiC MOSFET-Based Power Module Design and Analysis for EV Traction Systems. In Proceedings of the 2018 IEEE Energy Conversion Congress and Exposition (ECCE), Portland, OR, USA, 23–27 September 2018.
65. Aranzabal, I.; de Alegria, I.M.; Delmonte, N.; Cova, P.; Kortabarria, I. Comparison of the Heat Transfer Capabilities of Conventional Single- and Two-Phase Cooling Systems for an Electric Vehicle IGBT Power Module. *IEEE Trans. Power Electron.* **2019**, *34*, 4185–4194. [CrossRef]
66. Mademlis, G.; Orbay, R.; Liu, Y.; Sharma, N.; Arvidsson, R.; Thiringer, T. Multidisciplinary cooling design tool for electric vehicle SiC inverters utilizing transient 3D-CFD computations. *eTransportation* **2021**, *7*, 100092. [CrossRef]
67. Ladeinde, F.; Muley, A.; Stoia, M.; Ek, G.; Alabi, K.; Li, W. Experimental measurements and mathematical modeling of cold plate for aviation thermal management. *Int. J. Heat Mass Transf.* **2022**, *191*, 122810. [CrossRef]
68. Raske, N.; Gonzalez, O.A.; Furino, S.; Pietropaoli, M.; Shahpar, S.; Montomoli, F. Thermal management for electrification in aircraft engines optimization of coolant system. In Proceedings of the ASME Turbo Expo 2022, Rotterdam, The Netherlands, 13–17 June 2022.
69. Puqi, N.; Zhenxian, L.; Wang, F. Power Module and Cooling System Thermal Performance Evaluation for HEV Application. *IEEE J. Emerg. Sel. Top. Power Electron.* **2014**, *2*, 487–495. [CrossRef]
70. Gillot, C.; Schaeffer, C.; Massit, C.; Meysenc, L. Double-sided cooling for high power IGBT modules using flip chip technology. *IEEE Trans. Compon. Packag. Technol.* **2001**, *24*, 698–704. [CrossRef]
71. Zhu, S.; Li, Y.; Wang, Y.; Ma, Y.; Wu, C.; Jiao, M.; Zhao, Z.; Yu, J. Advanced double sided cooling IGBT module and power control unit development. In Proceedings of the 2017 IEEE International Workshop on Integrated Power Packaging (IWIPP), Delft, The Netherlands, 5–7 April 2017.
72. Liu, C.-K.; Wu, S.-T.; Lo, Y.-Y.; Chiu, P.-K.; Lin, H.-H.; Chen, Y.-S.; Tzeng, C.-M. Double-Sided Cooling SiC Power Module Packaging for Industrial Motor Driving System. In Proceedings of the 15th International Microsystems, Packaging, Assembly and Circuits Technology Conference (IMPACT), Taipei, Taiwan, 21–23 October 2020.
73. Becker, N.; Bulovic, S.; Bittner, R.; Herzer, R. Thermal Simulation for Power Density Optimization of SiC-MOSFET Automotive Inverter. In Proceedings of the 11th International Conference on Integrated Power Electronics Systems, Berlin, Germany, 24–26 March 2020.
74. Liu, C.-K.; Chiu, P.-K.; Hsu, S.-F.; Wu, H.-L.; Wu, S.-T.; Lai, W.-S.; Liu, H.-H.; Lee, M.-T. Effects of Thermal Characteristics of Power Module on Electric Vehicle Inverter. In Proceedings of the 2021 16th International Microsystems, Packaging, Assembly and Circuits Technology Conference (IMPACT), Taipei, Taiwan, 21–23 December 2021; pp. 143–146.
75. Fan, X.J.; Zhong, F.Q.; Yu, G.; Li, J.G.; Sung, C.J. Catalytic Cracking and Heat Sink Capacity of Aviation Kerosene Under Supercritical Conditions. *J. Propuls. Power* **2009**, *25*, 1226–1232. [CrossRef]
76. Fan, S.; Duan, F. A review of two-phase submerged boiling in thermal management of electronic cooling. *Int. J. Heat Mass Transf.* **2020**, *150*, 119324. [CrossRef]
77. Jackson, S.D.; Palazotto, A.N.; Pachter, M.; Niedbalski, N. Control of Vapor Compression Cycles under Transient Thermal Loads. In Proceedings of the AIAA Scitech 2019 Forum, San Diego, CA, USA, 7–11 January 2019.
78. Nonneman, J.; Schlimpert, S.; T'Jollyn, I.; Sergeant, P.; Paepe, M.D. Experimental Investigation of Direct Contact Baseplate Cooling for Electric Vehicle Power Electronics. In Proceedings of the 2019 18th IEEE Intersociety Conference on Thermal and Thermomechanical Phenomena in Electronic Systems (ITherm), Las Vegas, NV, USA, 28–31 May 2019.
79. Nonneman, J.; T'Jollyn, I.; Clarie, N.; Weckx, S.; Sergeant, P.; Paepe, M.D. Model-Based Comparison of Thermo-Hydraulic Performance of Various Cooling Methods for Power Electronics of Electric Vehicles. In Proceedings of the 17th IEEE Intersociety Conference on Thermal and Thermomechanical Phenomena in Electronic Systems (ITherm), San Diego, CA, USA, 29 May–1 June 2018.
80. Wang, Y.; Jones, S.; Dai, A.; Liu, G. Reliability enhancement by integrated liquid cooling in power IGBT modules for hybrid and electric vehicles. *Microelectron. Reliab.* **2014**, *54*, 1911–1915. [CrossRef]
81. Xu, Z.; Xu, F.; Jiang, D.; Cao, W.; Wang, F. A high temperature traction inverter with reduced cooling and improved efficiency for HEV applications. In Proceedings of the 2013 IEEE Energy Conversion Congress and Exposition, Denver, CO, USA, 15–19 September 2013.
82. Jung, K.W.; Kharangate, C.R.; Lee, H.; Palko, J.; Zhou, F.; Asheghi, M.; Dede, E.M.; Goodson, K.E. Microchannel cooling strategies for high heat flux (1 kW cm2) power electronic applications. In Proceedings of the 2017 16th IEEE Intersociety Conference on Thermal and Thermomechanical Phenomena in Electronic Systems (ITherm), Orlando, FL, USA, 30 May–2 June 2017.
83. Uhleman, A.; Hymon, E. Directly Cooled HybridPACK Power Modules with Ribbon Bonded Cooling Structures. In Proceedings of the PCIM Europe 2018, Nuremberg, Germany, 5–7 June 2018.

84. Jung, K.W.; Kharangate, C.R.; Lee, H.; Palko, J.; Zhou, F.; Asheghi, M.; Dede, E.M.; Goodson, K.E. Embedded cooling with 3D manifold for vehicle power electronics application: Single-phase thermal-fluid performance. *Int. J. Heat Mass Transf.* **2019**, *130*, 1108–1119. [CrossRef]
85. Hou, F.; Wang, W.; Zhang, H.; Chen, C.; Chen, C.; Lin, T.; Cao, L.; Zhang, G.Q.; Ferreira, J.A. Experimental evaluation of a compact two-phase cooling system for high heat flux electronic packages. *Appl. Therm. Eng.* **2019**, *163*, 114338. [CrossRef]
86. Hou, F.; Zhang, H.; Huang, D.; Fan, J.; Liu, F.; Lin, T.; Cao, L.; Fan, X.; Ferreira, J.A.; Zhang, G. Microchannel Thermal Management System with Two-Phase Flow for Power Electronics over 500 W/cm2 Heat Dissipation. *IEEE Trans. Power Electron.* **2020**, *35*, 10592–10600. [CrossRef]
87. Yuki, K.; Kibushi, R.; Tsuji, R.; Takai, K.; Unno, N.; Ogushi, T.; Murakami, M.; Numata, T.; Nomura, H.; Ide, T. Thermal management of automotive SiC-based on-board inverter with 500 W/cm^2 in heat flux, and Two-phase immersion cooling by breathing phenomenon spontaneously induced by lotus porous copper jointed onto a grooved heat transfer surface. *J. Therm. Sci. Technol.* **2020**, *15*, 1–11. [CrossRef]
88. Shi, M.; Yu, X.; Tan, Y.; Wang, X.; Zhang, X.; Li, J. Thermal performance of insulated gate bipolar transistor module using microchannel cooling base plate. *Appl. Therm. Eng.* **2022**, *201*, 117718. [CrossRef]
89. Xu, Z.; Xu, F.; Ning, P.; Wang, F. Development of a 30 kW Si IGBT based three-phase converter for operation at 200 °C with high temperature coolant in hybrid electric vehicle applications. In Proceedings of the 2013 Twenty-Eighth Annual IEEE Applied Power Electronics Conference and Exposition (APEC), Long Beach, CA, USA, 17–21 March 2013.
90. T'Jollyn, I.; Nonneman, J.; Beyne, W.; De Paepe, M. Nucleate pool boiling heat transfer and critical heat flux of FK-649 on an inverter power module. *Heat Mass Transf.* **2022**, *15*, 1–8. [CrossRef]
91. Nadda, R.; Kumar, A.; Maithani, R. Efficiency improvement of solar photovoltaic/solar air collectors by using impingement jets: A review. *Renew. Sustain. Energy Rev.* **2018**, *93*, 331–353. [CrossRef]
92. Devahdhanush, V.S.; Mudawar, I. Review of Critical Heat Flux (CHF) in Jet Impingement Boiling. *Int. J. Heat Mass Transf.* **2021**, *169*, 120893. [CrossRef]
93. Eng Ewe, W.; Fudholi, A.; Sopian, K.; Solomin, E.; Hossein Yazdi, M.; Asim, N.; Fatima, N.; Pikra, G.; Sudibyo, H.; Fatriasari, W.; et al. Jet impingement cooling applications in solar energy technologies: Systematic literature review. *Therm. Sci. Eng. Prog.* **2022**, *34*, 101445. [CrossRef]
94. Ekkad, S.V.; Parida, P.; Ngo, K. High Efficiency Minichannel and Mini-Impingement Cooling Systems for Hybrid Electric Vehicle Electronics. In Proceedings of the ASME 2012 10th International Conference on Nanochannels, Microchannels, and Minichannels, Rio Grande, Puerto Rico, 8–12 July 2012.
95. Gould, K.; Cai, Q.S.; Neft, C.; Bhunia, A. Thermal management of silicon carbide power module for military hybrid vehicles. In Proceedings of the 2014 Semiconductor Thermal Measurement and Management Symposium (SEMI-THERM), San Jose, CA, USA, 9–13 March 2014.
96. Bhunia, A.; Chen, C.-L. Jet impingement cooling of an inverter module in the harsh environment of a hybrid vehicle. In Proceedings of the 2005 ASME Summer Heat Transfer Conference, San Francisco, CA, USA, 17–22 July 2005.
97. Tang, G.; Wai, L.C.; Boon Lim, S.; Lau, B.L.; Kazunori, Y.; Zhang, X.W. Thermal Analysis, Characterization and and Material Selection for SiC Device Based Intelligent Power Module (IPM). In Proceedings of the 2020 IEEE 70th Electronic Components and Technology Conference (ECTC), Orlando, FL, USA, 3–30 June 2020; pp. 2078–2085.
98. Moreno, G.; Narumanchi, S.; Tomerlin, J.; Major, J. Single-Phase Dielectric Fluid Thermal Management for Power-Dense Automotive Power Electronics. *IEEE Trans. Power Electron.* **2022**, *37*, 12474–12485. [CrossRef]
99. Pourfattah, F.; Sabzpooshani, M. On the thermal management of a power electronics system: Optimization of the cooling system using genetic algorithm and response surface method. *Energy* **2021**, *232*, 120951. [CrossRef]
100. Zaman, M.S.; Michalak, A.; Nasr, M.; Silva, C.d.; Mills, J.K.; Amon, C.H.; Trescases, O. Multiphysics Optimization of Thermal Management Designs for Power Electronics Employing Impingement Cooling and Stereolithographic Printing. *IEEE Trans. Power Electron.* **2021**, *36*, 12769–12780. [CrossRef]
101. Jones-Jackson, S.; Azer, P.; Emadi, A. Improved Thermal Management of Power Modules at Transient Heat Loading using Jet Impingement. In Proceedings of the 2022 IEEE Transportation Electrification Conference & Expo (ITEC), Anaheim, CA, USA, 15–17 June 2022; pp. 180–184.
102. Chen, H.; Ruan, X.-H.; Peng, Y.-H.; Wang, Y.-L.; Yu, C.-K. Application status and prospect of spray cooling in electronics and energy conversion industries. *Sustain. Energy Technol. Assess.* **2022**, *52*, 102181. [CrossRef]
103. Liang, G.; Mudawar, I. Review of spray cooling—Part 1: Single-phase and nucleate boiling regimes, and critical heat flux. *Int. J. Heat Mass Transf.* **2017**, *115*, 1174–1205. [CrossRef]
104. Liang, G.; Mudawar, I. Review of spray cooling—Part 2: High temperature boiling regimes and quenching applications. *Int. J. Heat Mass Transf.* **2017**, *115*, 1206–1222. [CrossRef]
105. Bostanci, H.; Ee, D.V.; Saarloos, B.A.; Rini, D.P.; Chow, L.C. Spray cooling of power electronics using high temperature coolant and enhanced surface. In Proceedings of the 2009 IEEE Vehicle Power and Propulsion Conference, Dearborn, MI, USA, 7–10 September 2009.
106. Mertens, R.G.; Chow, L.; Sundaram, K.B.; Cregger, R.B.; Rini, D.P.; Turek, L.; Saarloos, B.A. Spray Cooling of IGBT Devices. *J. Electron. Packag.* **2007**, *129*, 316–323. [CrossRef]

107. Mudawar, I.; Bharathan, D.; Kelly, K.; Narumanchi, S. Two-Phase Spray Cooling of Hybrid Vehicle Electronics. *IEEE Trans. Compon. Packag. Technol.* **2009**, *32*, 501–512. [CrossRef]
108. Turek, L.J.; Rini, D.P.; Saarloos, B.A.; Chow, L.C. Evaporative spray cooling of power electronics using high temperature coolant. In Proceedings of the 2008 11th Intersociety Conference on Thermal and Thermomechanical Phenomena in Electronic Systems, Orlando, FL, USA, 28–31 May 2008.
109. Turek, L.J.; Rini, D.P.; Saarloos, B.A.; Chow, L.C. Enabling Much Higher Power Densities in Aerospace Power Electronics with High Temperature Evaporative Spray Cooling. In Proceedings of the Power Systems Conference, Bellevue, WA, USA, 11–13 November 2008.
110. Riaz Siddiqui, F.; Tso, C.-Y.; Qiu, H.; Chao, C.Y.H.; Chung Fu, S. Hybrid nanofluid spray cooling performance and its residue surface effects: Toward thermal management of high heat flux devices. *Appl. Therm. Eng.* **2022**, *211*, 118454. [CrossRef]
111. Bostanci, H.; Van Ee, D.; Saarloos, B.A.; Rini, D.P.; Chow, L.C. Thermal Management of Power Inverter Modules at High Fluxes via Two-Phase Spray Cooling. *IEEE Trans. Compon. Packag. Manuf. Technol.* **2012**, *2*, 1480–1485. [CrossRef]
112. Bostanci, H.; Altalidi, S.S.; Nasrazadani, S. Two-phase spray cooling with HFC-134a and HFO-1234yf on practical enhanced surfaces. *Appl. Therm. Eng.* **2018**, *131*, 150–158. [CrossRef]
113. Xu, R.; Wang, G.; Jiang, P. Spray Cooling on Enhanced Surfaces: A Review of the Progress and Mechanisms. *J. Electron. Packag.* **2022**, *144*, 010802. [CrossRef]
114. Panão, M.R.O.; Correia, A.M.; Moreira, A.L.N. High-power electronics thermal management with intermittent multijet spray. *Appl. Therm. Eng.* **2012**, *37*, 293–301. [CrossRef]
115. Xu, X.; Wang, Y.; Jiang, Y.; Liu, J.; Yuan, X. Recent Advances in Closed Loop Spray Cooling and its Application in Airborne Systems. *J. Therm. Sci.* **2020**, *30*, 32–50. [CrossRef]
116. Wang, J.-X.; Guo, W.; Xiong, K.; Wang, S.-N. Review of aerospace-oriented spray cooling technology. *Prog. Aerosp. Sci.* **2020**, *116*, 100635. [CrossRef]
117. Venkategowda, Y.T.; Jafari, S.; Nikolaidis, T. Thermal Management System Design for More Electric Aircraft Avionics using Evaporative Spray Cooling. In Proceedings of the Global Power and Propulsion Society, Chania, Greece, 7–9 September 2020.
118. Van Heerden, A.S.J.; Judt, D.M.; Jafari, S.; Lawson, C.P.; Nikolaidis, T.; Bosak, D. Aircraft thermal management: Practices, technology, system architectures, future challenges, and opportunities. *Prog. Aerosp. Sci.* **2022**, *128*, 100767. [CrossRef]
119. Mochizuki, M. Latest development and application of heat pipes for electronics and automotive. In Proceedings of the 2017 IEEE CPMT Symposium Japan (ICSJ), Kyoto, Japan, 20–22 November 2017.
120. Chen, X.; Ye, H.; Fan, X.; Ren, T.; Zhang, G. A review of small heat pipes for electronics. *Appl. Therm. Eng.* **2016**, *96*, 1–17. [CrossRef]
121. Singh, R.; Mochizuki, M.; Saito, Y.; Yamada, T.; Nguyen, T.; Nguyen, T. Heat pipe applications in cooling automotive electronics. *Heat Pipe Sci. Technol. Int. J.* **2016**, *7*, 57–69. [CrossRef]
122. Zaghdoudi, M.C.; Teytu, A. Use of heat pipes for avionics cooling. In Proceedings of the 3rd Electronics Packaging Technology Conference (EPTC 2000), Singapore, 7 December 2000.
123. Cai, Q.; Chen, C.-l.; Asfia, J.F. Experimental Investigations of an Avionics Cooling System for Aerospace Vehicle. *J. Spacecr. Rocket.* **2007**, *44*, 439–444. [CrossRef]
124. Singh, R.; Akbarzadeh, A.; Mochizuki, M. Thermal Performance of a Capillary Pumped Loop for Automotive Cooling. *Exp. Heat Transf.* **2008**, *21*, 296–313. [CrossRef]
125. Anderson, W.G.; Hartenstine, J.; Ellis, M.; Montgomery, J.; Peters, C. Electronics Cooling Using High Temperature Loop Heat Pipes with Multiple Condensers. In Proceedings of the SAE Power Systems Conference, Worth, TX, USA, 2–4 November 2010.
126. Reyes, M.; Alonso, D.; Arias, J.R.; Velazquez, A. Experimental and theoretical study of a vapour chamber based heat spreader for avionics applications. *Appl. Therm. Eng.* **2012**, *37*, 51–59. [CrossRef]
127. Burban, G.; Ayel, V.; Alexandre, A.; Lagonotte, P.; Bertin, Y.; Romestant, C. Experimental investigation of a pulsating heat pipe for hybrid vehicle applications. *Appl. Therm. Eng.* **2013**, *50*, 94–103. [CrossRef]
128. Jones, A.B.; Chen, R. Experimental Assessment of Vapour Chamber Heater Spreader Implementation in Avionic Cooling. In Proceedings of the 53rd AIAA Aerospace Sciences Meeting, Kissimmee, FL, USA, 5–9 January 2015.
129. Cai, S.Q.; Bhunia, A.; Asfia, J.F. A Passive and Remote Heat Transfer Solution for Avionics Thermal Management. *J. Therm. Sci. Eng. Appl.* **2017**, *9*, 021009. [CrossRef]
130. Tecchio, C.; Paiva, K.V.; Oliveira, J.L.G.; Mantelli, M.B.H.; Gandolfi, R.; Ribeiro, L.G.S. Passive cooling concept for onboard heat sources in aircrafts. *Exp. Therm. Fluid Sci.* **2017**, *82*, 402–413. [CrossRef]
131. Zilio, C.; Righetti, G.; Mancin, S.; Hodot, R.; Sarno, C.; Pomme, V.; Truffart, B. Active and passive cooling technologies for thermal management of avionics in helicopters: Loop heat pipes and mini-Vapor Cycle System. *Therm. Sci. Eng. Prog.* **2018**, *5*, 107–116. [CrossRef]
132. Accorinti, F.; Erroui, N.; Ayel, V.; Gateau, G.; Bertin, Y.; Roux, N.; Dutour, S.; Miscevic, M. High-efficiency cooling system for highly integrated power electronics for hybrid propulsion aircraft. In Proceedings of the 2019 IEEE 28th International Symposium on Industrial Electronics (ISIE), Vancouver, BC, Canada, 12–14 June 2019; pp. 870–877.
133. Chen, Y.; Li, B.; Wang, X.; Yan, Y.; Wang, Y.; Qi, F. Investigation of heat transfer and thermal stresses of novel thermal management system integrated with vapour chamber for IGBT power module. *Therm. Sci. Eng. Prog.* **2019**, *10*, 73–81. [CrossRef]

134. Chen, Y.; Yan, Y.; Li, B. Thermal Analyses of Power Electronics Integrated with Vapour Chamber Cooling. *Automot. Innov.* **2020**, *3*, 328–335. [CrossRef]
135. Li, B.; Chen, Y.; Wang, X.; Li, Y.; Yan, Y. Heat spreading performance of SiC-based power module with bonded vapour chamber for electric powertrain integration. *Appl. Therm. Eng.* **2020**, *181*, 115896. [CrossRef]
136. Junior, A.A.M.; Mantelli, M.B.H. Thermal performance of a novel flat thermosyphon for avionics thermal management. *Energy Convers. Manag.* **2019**, *202*, 112219. [CrossRef]
137. Simas, G.V.; Mera, J.P.F.; Mantelli, M.B.H. Study of a Loop Thermosyphon Evaporator for Thermal Control of Aircrafts. *J. Heat Transf.* **2019**, *141*, 091812. [CrossRef]
138. Pagnoni, F.; Ayel, V.; Bertin, Y.; Coulloux, J.; Zebian, M. Loop Heat Pipe for Thermal Management of Aircraft Engine Equipment. *J. Thermophys. Heat Transf.* **2021**, *35*, 323–334. [CrossRef]
139. Dreiling, R.; Zimmermann, S.; Nguyen-Xuan, T.; Schreivogel, P.; di Mare, F. Thermal Management based on Flat-Plate Pulsating Heat Pipes for Power Modules of Electric Powertrains. In Proceedings of the 2022 IEEE Transportation Electrification Conference & Expo (ITEC), Anaheim, CA, USA, 15–17 June 2022; pp. 819–824.
140. Singh, R.; Nguyen, T. Loop Heat Pipes for Thermal Management of Electric Vehicles. *J. Therm. Sci. Eng. Appl.* **2022**, *14*, 061010. [CrossRef]
141. Maydanik, Y.F. Loop heat pipes. *Appl. Therm. Eng.* **2005**, *25*, 635–657. [CrossRef]
142. Nakamura, K.; Odagiri, K.; Nagano, H. Study on a loop heat pipe for a long-distance heat transport under anti-gravity condition. *Appl. Therm. Eng.* **2016**, *107*, 167–174. [CrossRef]
143. Lian, W.; Niu, W.; Lin, L. A passive cooling design for an aircraft electromechanical actuator by using heat pipes. *Appl. Therm. Eng.* **2021**, *184*, 116248. [CrossRef]
144. Passive Cooling Solution Validation for Aircraft Application. Available online: https://cordis.europa.eu/project/id/323528/reporting (accessed on 1 August 2022).
145. Accorinti, F.; Ayel, V.; Bertin, Y. Steady-state analysis of a Capillary Pumped Loop for Terrestrial Application with methanol and ethanol as working fluids. *Int. J. Therm. Sci.* **2019**, *137*, 571–583. [CrossRef]
146. Ayel, V.; Accorinti, F.; Dutour, S.; Bertin, Y. Thermal management & advanced cooling technologies of power electronics converters for hybrid aircraft applications. In Proceedings of the MEA2021—More Electric Aircraft—Towards cleaner Aviation, Bordeaux, France, 24 September 2021.
147. Su, Q.; Chang, S.; Zhao, Y.; Zheng, H.; Dang, C. A review of loop heat pipes for aircraft anti-icing applications. *Appl. Therm. Eng.* **2018**, *130*, 528–540. [CrossRef]
148. Hua, W.; Zhang, L.; Zhang, X. Research on passive cooling of electronic chips based on PCM: A review. *J. Mol. Liq.* **2021**, *340*, 117183. [CrossRef]
149. Bianco, V.; De Rosa, M.; Vafai, K. Phase-change materials for thermal management of electronic devices. *Appl. Therm. Eng.* **2022**, *214*, 118839. [CrossRef]
150. Tang, X.; Bonner, R.; Desai, T.; Fan, A. A 2-D numerical study of microscale phase change material thermal storage for GaN transistor thermal management. In Proceedings of the 27th Annual IEEE Semiconductor Thermal Measurement and Management Symposium, San Jose, CA, USA, 20–24 March 2011.
151. Orr, B.G.; Singh, R.; Phan, T.-L.; Mochizuki, M. Transient Modelling of an Ev Inverter Heat Sink with PCM. *Front. Heat Mass Transf.* **2019**, *13*, 1–6. [CrossRef]
152. Boteler, L.; Niedbalski, N.; Choi, S.; Lundh, J.S.; Shamberger, P.; Huitink, D.; de Bock, H.P. A System to Package Perspective on Transient Thermal Management of Electronics. *J. Electron. Packag.* **2020**, *142*, 041111. [CrossRef]
153. Hartsfield, C.R.; Shelton, T.E.; Palmer, B.O.; O'Hara, R. All-Metallic Phase Change Thermal Management Systems for Transient Spacecraft Loads. *J. Aerosp. Eng.* **2020**, *33*, 04020039. [CrossRef]
154. Pal, D.; Joshi, Y.K. Thermal Management of an Avionics Module Using Solid-Liquid Phase-Change Materials. *J. Thermophys. Heat Transf.* **1998**, *12*, 256–262. [CrossRef]
155. Fossett, A.J.; Maguire, M.T.; Kudirka, A.A.; Mills, F.E.; Brown, D.A. Avionics Passive Cooling with Microencapsulated Phase Change Materials. *Trans. ASME* **1998**, *120*, 238–242. [CrossRef]
156. Nafis, B.M.; Iradukunda, A.C.; Huitink, D. System-Level Thermal Management and Reliability of Automotive Electronics: Goals and Opportunities Using Phase-Change Materials. *J. Electron. Packag.* **2020**, *142*, 041108. [CrossRef]
157. Ibrahim, N.I.; Al-Sulaiman, F.A.; Rahman, S.; Yilbas, B.S.; Sahin, A.Z. Heat transfer enhancement of phase change materials for thermal energy storage applications: A critical review. *Renew. Sustain. Energy Rev.* **2017**, *74*, 26–50. [CrossRef]
158. Ghosh, D.; Ghose, J.; Datta, P.; Kumari, P.; Paul, S. Strategies for phase change material application in latent heat thermal energy storage enhancement: Status and prospect. *J. Energy Storage* **2022**, *53*, 105179. [CrossRef]
159. Liu, C.; Rao, Z.; Zhao, J.; Huo, Y.; Li, Y. Review on nanoencapsulated phase change materials: Preparation, characterization and heat transfer enhancement. *Nano Energy* **2015**, *13*, 814–826. [CrossRef]
160. Tariq, S.L.; Ali, H.M.; Akram, M.A.; Janjua, M.M.; Ahmadlouydarab, M. Nanoparticles enhanced phase change materials (NePCMs)—A recent review. *Appl. Therm. Eng.* **2020**, *176*, 115305. [CrossRef]
161. Saha, S.K.; Dutta, P.; Paruya, S.; Kar, S.; Roy, S. Cooling of Electronics with Phase Change Materials. *AIP Conf. Proc.* **2010**, *1298*, 31–36. [CrossRef]

162. Wu, B.; Li, P.; Zhang, F.; Tian, F. A novel phase change material-based heat sink with an orthotropic plate to enhance the temperature field uniformity for avionics. *J. Mech. Sci. Technol.* **2021**, *35*, 2237–2246. [CrossRef]
163. Li, D.; Yang, X.; Wang, S.; Duan, D.; Wan, Z.; Xia, G.; Liu, W. Experimental research on vibration-enhanced heat transfer of fin-tube vehicle radiator. *Appl. Therm. Eng.* **2020**, *180*, 115836. [CrossRef]
164. Fu, J.; Miao, X.; Zuo, Q.; Tang, H.; Li, Y.; Zhang, Y.; Sunden, B. Heat transfer and field synergy characteristics in a rectangular unit channel under mechanical vibration. *Int. Commun. Heat Mass Transf.* **2022**, *136*, 106176. [CrossRef]
165. Haji Hosseinloo, A.; Tan, S.P.; Yap, F.F.; Toh, K.C. Shock and vibration protection of submerged jet impingement cooling systems: Theory and experiment. *Appl. Therm. Eng.* **2014**, *73*, 1076–1086. [CrossRef]
166. Wang, Z.; Xing, Y.; Liu, X.; Zhao, L.; Ji, Y. Computer modeling of droplets impact on heat transfer during spray cooling under vibration environment. *Appl. Therm. Eng.* **2016**, *107*, 453–462. [CrossRef]
167. Hsu, C.-C.; Chen, X.-F.; Yang, J.-M. The Effects of Shock and Vibration on Heat Pipe Performance in Reliability Tests. In Proceedings of the 10th International Heat Pipe Symposium, Taipei, Taiwan, 6–9 November 2011.
168. Alaei, A.; Kafshgari, M.H.; Rahimi, S.K. A vertical heat pipe: An experimental and statistical study of the thermal performance in the presence of low-frequency vibrations. *Heat Mass Transf.* **2012**, *49*, 285–290. [CrossRef]
169. Kumar, P.; Khandekar, S.; Maydanik, Y.F.; Bhattacharya, B. Effect of Vibrations on Thermal Performance of Miniature Loop Heat Pipe for Avionics Cooling: An Experimental Analysis. *J. Heat Transf.* **2019**, *141*, 091814. [CrossRef]
170. Wu, Y.; Zhang, X.; Xu, X.; Lin, X.; Liu, L. A review on the effect of external fields on solidification, melting and heat transfer enhancement of phase change materials. *J. Energy Storage* **2020**, *31*, 101567. [CrossRef]
171. Joshy, N.; Hajiyan, M.; Siddique, A.R.M.; Tasnim, S.; Simha, H.; Mahmud, S. Experimental investigation of the effect of vibration on phase change material (PCM) based battery thermal management system. *J. Power Sources* **2020**, *450*, 227717. [CrossRef]
172. Wu, G.; Chen, S.; Zeng, S. Effects of mechanical vibration on melting behaviour of phase change material during charging process. *Appl. Therm. Eng.* **2021**, *192*, 116914. [CrossRef]
173. Zhang, W.; Li, X.; Wu, W.; Huang, J. Influence of mechanical vibration on composite phase change material based thermal management system for lithium-ion battery. *J. Energy Storage* **2022**, *54*, 105237. [CrossRef]
174. Zhao, X.; Zhang, B.; Yang, Z.; Zhao, Y. Surface orientation effects on heat transfer performance of spray cooling. *Int. J. Heat Mass Transf.* **2020**, *147*, 118960. [CrossRef]
175. Ku, J.; Ottenstein, L.; Kaya, T.; Rogers, P.; Hoff, C. Testing of A Loop Heat Pipe Subjected to Variable Accelerating Forces, Part 1: Start-up. In Proceedings of the 30th International Conference on Environmental Systems, Toulouse, France, 10–13 July 2000.
176. Ku, J.; Ottenstein, L.; Kaya, T.; Rogers, P.; Hoff, C. Testing of A Loop Heat Pipe Subjected to Variable Accelerating Forces, Part 2: Temperature Stability. In Proceedings of the 30th International Conference on Environmental Systems, Toulouse, France, 10–13 July 2000.
177. Fleming, A.J.; Thomas, S.K.; Yerkes, K.L. Titanium-Water Loop Heat Pipe Operating Characteristics Under Standard and Elevated Acceleration Fields. *J. Thermophys. Heat Transf.* **2010**, *24*, 184–198. [CrossRef]
178. Xie, Y.; Zhang, J.; Xie, L.; Yu, Y.; Wu, H.; Zhang, H.; Gao, H. Experimental investigation on the operating characteristics of a dual compensation chamber loop heat pipe subjected to acceleration field. *Appl. Therm. Eng.* **2015**, *81*, 297–312. [CrossRef]
179. Xie, Y.; Zhou, Y.; Wen, D.; Wu, H.; Haritos, G.; Zhang, H. Experimental investigation on transient characteristics of a dual compensation chamber loop heat pipe subjected to acceleration forces. *Appl. Therm. Eng.* **2018**, *130*, 169–184. [CrossRef]
180. Xie, Y.; Li, X.; Dong, S.; Zhang, H.; Wu, H. Experimental investigation on operating behaviors of loop heat pipe with thermoelectric cooler under acceleration conditions. *Chin. J. Aeronaut.* **2020**, *33*, 852–860. [CrossRef]
181. Nagano, H.; Ku, J. Gravity Effect on Capillary Limit in a Miniature Loop Heat Pipe with Multiple Evaporators and Multiple Condensers. *AIP Conf. Proc.* **2007**, *880*, 3–10.
182. Liu, W.; Gou, J.; Luo, Y.; Zhang, M. The experimental investigation of a vapor chamber with compound columns under the influence of gravity. *Appl. Therm. Eng.* **2018**, *140*, 131–138. [CrossRef]
183. Xu, Y.; Wang, J.; Yan, Z. Experimental investigation on melting heat transfer characteristics of a phase change material under hypergravity. *Int. J. Heat Mass Transf.* **2021**, *181*, 122004. [CrossRef]
184. Xu, Y.; Wang, J.; Li, T. Experimental study on the heat transfer performance of a phase change material based pin-fin heat sink for heat dissipation in airborne equipment under hypergravity. *J. Energy Storage* **2022**, *52*, 104742. [CrossRef]
185. Tang, J.; Xie, Y.; Chang, S.; Yan, Z.; Wu, H.; Zhang, H. Performance analysis of acceleration effect on paraffin melting in finned copper foam. *Appl. Therm. Eng.* **2022**, *202*, 117826. [CrossRef]